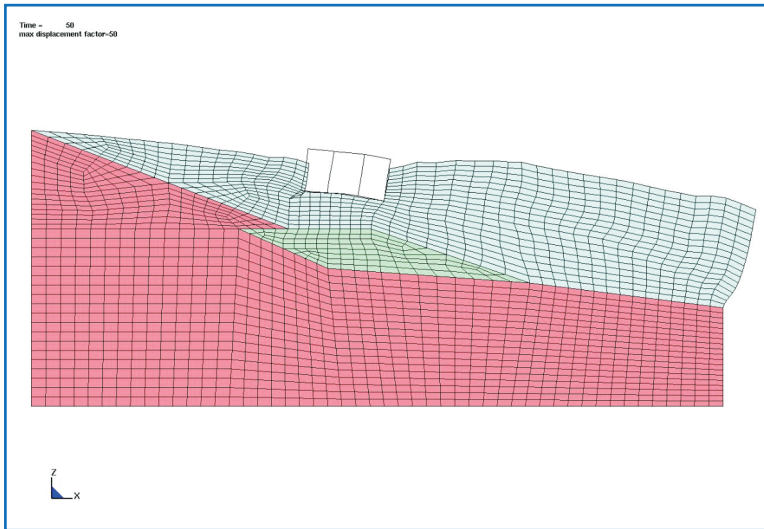


RECLAMATION

Managing Water in the West

Report DSO-06-01

Computer Material Models for Soils using FLAC and DYNA



Dam Safety Technology Development Program



U.S. Department of the Interior
Bureau of Reclamation
Technical Service Center
Denver, Colorado

May 2006

REPORT DOCUMENTATION PAGE

*Form Approved
OMB No. 0704-0188*

The public reporting burden for this collection of information is estimated to average 1 hour per response, including the time for reviewing instructions, searching existing data sources, gathering and maintaining the data needed, and completing and reviewing the collection of information. Send comments regarding this burden estimate or any other aspect of this collection of information, including suggestions for reducing the burden, to Department of Defense, Washington Headquarters Services, Directorate for Information Operations and Reports (0704-0188), 1215 Jefferson Davis Highway, Suite 1204, Arlington, VA 22202-4302. Respondents should be aware that notwithstanding any other provision of law, no person shall be subject to any penalty for failing to comply with a collection of information if it does not display a currently valid OMB control number.

PLEASE DO NOT RETURN YOUR FORM TO THE ABOVE ADDRESS.

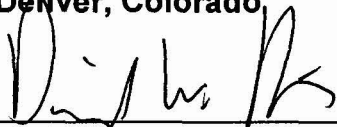
1. REPORT DATE (DD-MM-YYYY) 05-2006		2. REPORT TYPE Technical		3. DATES COVERED (From - To)	
4. TITLE AND SUBTITLE Computer Material Models for Soils, Rock, and Concrete Using FLAC and DYNA				5a. CONTRACT NUMBER	
				5b. GRANT NUMBER	
				5c. PROGRAM ELEMENT NUMBER	
6. AUTHOR(S) Harris, David W., PhD, PE				5d. PROJECT NUMBER	
				5e. TASK NUMBER	
				5f. WORK UNIT NUMBER	
7. PERFORMING ORGANIZATION NAME(S) AND ADDRESS(ES) Bureau of Reclamation Materials Engineering and Research Group PO Box 25007 Denver CO 80225				8. PERFORMING ORGANIZATION REPORT NUMBER DSO-06-01	
9. SPONSORING/MONITORING AGENCY NAME(S) AND ADDRESS(ES) Bureau of Reclamation Denver, Colorado				10. SPONSOR/MONITOR'S ACRONYM(S) USBR	
				11. SPONSOR/MONITOR'S REPORT NUMBER(S) DSO-06-01	
12. DISTRIBUTION/AVAILABILITY STATEMENT National Technical Information Service, 5285 Port Royal Road, Springfield, VA 22161					
13. SUPPLEMENTARY NOTES					
14. ABSTRACT This report summarizes material models available for the analysis of soils in the computer codes, FLAC and DYNA. The input constants needed for these models are emphasized. Typical values or ranges of values are given, and methods to calculate the parameters from laboratory data are discussed. In addition, dynamic damping in computations is discussed. Two components, mass (structural inertia) and stiffness (material hysteresis), are discussed. Field-measured values are presented and methods to calculate material damping in the lab shown. The report concludes that nonlinear analyses can be used to better understand complex site response of dams; models are available for these analyses. It is recommended that measured values from the structure in question be used for analyses.					
15. SUBJECT TERMS computer analysis, nonlinear analysis, dynamic analysis, embankment analysis, earthquake analysis, material modeling, embankment materials, laboratory testing, structural damping, material damping, embankment damping					
16. SECURITY CLASSIFICATION OF:			17. LIMITATION OF ABSTRACT SAR	18. NUMBER OF PAGES 53	19a. NAME OF RESPONSIBLE PERSON
a. REPORT U	b. ABSTRACT U	a. THIS PAGE U			19b. TELEPHONE NUMBER (Include area code)

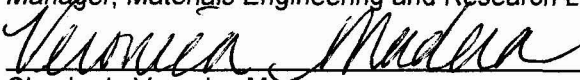
BUREAU OF RECLAMATION
Technical Service Center, Denver, Colorado
Materials Engineering and Research Laboratory, 86-68180

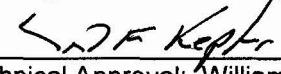
Report DSO-06-01

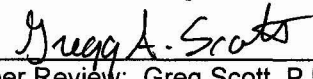
**Computer Material Models for Soils, Rock,
and Concrete Using FLAC and DYNA**

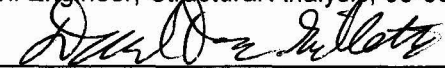
Dam Safety Technology Development Program
Denver, Colorado


Prepared: David W. Harris, Ph.D., P.E.
Manager, Materials Engineering and Research Laboratory, 86-68180


Checked: Veronica Madera
Civil Engineer, Materials Engineering and Research Laboratory, 86-68180


Technical Approval: William Kepler, Ph.D., P.E.
Research Civil Engineer, Materials Engineering and Research Laboratory, 86-68180


Peer Review: Greg Scott, P.E. 2/26/2007
Date
Civil Engineer, Structural Analysis, 86-68110


Peer Review: Dave Gillette, Ph.D., P.E. 2/26/07
Date
Civil Engineer, Geotechnical Engineering, 86-68313

REVISIONS					
Date	Description	Prepared	Checked	Technical Approval	Peer Review
3/6/06	Final revisions	X	X	X	X

Mission Statements

The mission of the Department of the Interior is to protect and provide access to our Nation's natural and cultural heritage and honor our trust responsibilities to Indian Tribes and our commitments to island communities.

The mission of the Bureau of Reclamation is to manage, develop, and protect water and related resources in an environmentally and economically sound manner in the interest of the American public.

Acknowledgement

Portions of the discussion of field measurements for FLAC properties were taken directly from drafts prepared by Leif Dixon, formerly of the Bureau of Reclamation.

Contents

	Page
Acknowledgement	iii
Introduction.....	1
FLAC-3D	2
Material Properties.....	2
Linear Elastic Properties	2
Stress-Dependent Properties	5
Intrinsic Strength Properties (Initiation of Failure)	5
Postfailure Properties	9
Shear Dilatancy.....	9
Shear Hardening/Softening.....	9
Tensile Softening	10
Large Strain Properties in FLAC	10
Liquefiable Strengths	14
Parameter and Testing Requirements for FLAC-3D	14
Calculation of Dynamic Pore Pressures.....	16
Finn and Byrne Models (Byrne, 1991)	17
User-Supplied Materials in FLAC	19
Hyperbolic Model	19
Other Hyperbolic Variations.....	20
Byrne Model	22
Strain Rate Effects	23
Recommendations for FLAC-3D Use	23
LS-DYNA.....	23
LS-DYNA Soil Material Models	24
Group 1 Models	24
#5, Soil and Foam	24
#25, Geologic Cap	24
#192, Soil Brick	25
#193, Drucker-Prager.....	25
Group 2 Models	25
#14, Soil and Foam w/ Failure.....	25
#78, Soil Concrete.....	25
#79, Elasto-Perfectly Plastic Soil.....	25
Group 3 Models	25
#16, Pseudo Geologic	25
#26, Honeycomb	25
#72, Concrete Damage.....	26
#96, Brittle Damage	26

Model 193 (from LS/DYNA3D Manual)—Detailed Description	26
Model 16 (from DYNA3D Manual)—Detailed Description.....	27
Response Mode I—Tabulated Yield Stress versus Pressure (Mohr-Coulomb)	27
Simple Tensile Failure	27
Response Mode II—Stress Strain Curve Input.....	27
Model 45 (DTRA Concrete/Geological Material)—Detailed Description.....	28
Equation of State.....	28
Plasticity Curves	29
Uniaxial Tension Strength	31
Damage Evolution	31
Shear Dilation	33
Element Elimination	33
Strain Rate Effects	33
LSDYNA or DYNA Dynamic Pore Pressure Calculations	35
Use of Damping in Analysis.....	36
Material Damping.....	37
Structural Damping.....	38
Conclusions and Recommendations	43
References.....	46

Tables

No.		Page
1	Selected elastic constants (laboratory-scale) for soil	3
2	Selected elastic constants (laboratory-scale) for rock.....	3
3	Estimating the Secant Modulus, E_s	6
4	Selected strength properties (laboratory-scale) for rock.....	7
5	Selected strength properties (drained, laboratory-scale) for soils.....	7
6	Selected other strength properties	8
7	Shear modulus and damping factors for soil classifications.....	11
8	FLAC properties and recommended tests.....	15
9	Typical hyperbolic constants	21
10	LS-DYNA/DYNA possible soil models.....	24
11	Typical values found for the a and b coefficients for WSMR and SAC concretes	33
12	Parameter and testing requirements for DYNA-3D.....	35
13	Estimated damping factors for prominent resonant frequencies.....	43

Figures

No.	Page
1	6
2	10
3	12
4	12
5	13
6	16
7	28
8	29
9	30
10	31
11	32
12	32
13	34
14	34
15	37
16	38
17	39
18	40
19	40
20	41
21	41
22	42
23	44
24	45

Introduction

Linear theory has been used extensively in structural analysis of soils and other materials. Linear analysis provides a needed first step in understanding a problem. Linear properties have been used in analysis and stresses compared to failure values. The inherent problem in this approach is that materials do not act in a linear fashion to their failure point. The approximation may be justified if the stresses in the soil mass are far from failure, if the changes in stress are small, and the magnitudes of the deformations are not of critical interest. Duncan (Duncan and Wong, 1999) observes that high accuracy is not expected from analyses in which soil and rock are represented solely as linear elastic materials. Such approximations may be justified if crude results are acceptable, although more judgment is required to interpret the results. Thus, the interpretation of stress values beyond proportional values requires either judgment and intuitive approaches, or the use of analysis capable of simulating nonlinear behavior.

In their Opinion Paper *Nonlinear Analysis for Site Response*, Makdisi and Wang (2004) state that nonlinear analyses provide a more realistic approach for evaluating the impact of strong ground shaking on soft, potentially liquefiable soils, and their effects on estimated ground motions on the surface of these deposits. Makdisi and Wang recommend that nonlinear analyses be encouraged and incorporated into the state of the practice for evaluating site response to better understand the uncertainties in nonlinear soil behavior and assess their impact on site response. Other observations on the need and use for nonlinear studies (Dakoulas and Gazetas, 1987) suggest that in the case of strong seismic excitation, soil nonlinearities aid in the reduction of peak crest accelerations due to increased hysteric damping and destruction of resonance through changes in stiffness characteristics. These effects drastically reduce the adverse effects of narrow canyon geometries on midcrest accelerations.

A number of computer codes are available for nonlinear analysis of soils. This report concentrates on two computer code series that at the time of writing of this document are considered codes for primary use at the Bureau of Reclamation: FLAC (Fast Lagrangian Analysis of Continua) 2D and 3D, and DYNA/LS-DYNA (Dynamic Nonlinear Analysis). In cases where the conditions stated above are not met, these codes should be used to characterize the stress-strain behavior and analysis of soils.

This report describes how to produce material properties for use in FLAC and DYNA. The measurement and use of these properties will allow the analysis of critical structures using nonlinear methods. This state-of-the-practice approach provides the best estimate of behavior given a known geometry, material

properties, discontinuities, and loading conditions. These estimates are used to make better evaluations and decisions concerning critical structures.

FLAC-3D

FLAC-3D is a three dimensional explicit finite-difference program for engineering mechanics computation. Each element behaves according to a prescribed linear or nonlinear stress/strain law in response to applied forces or boundary restraints. The material can yield and flow, and the grid can deform (in large strain mode) and move with the material that is represented.

Material Properties

The following linear elastic, initiation of failure (nonlinear), and postfailure modes are available in FLAC-3D.

Linear Elastic Properties

All materials models in FLAC-3D, except the transversely isotropic elastic and orthotropic elastic models, assume isotropic material behavior in the elastic range described by two elastic constants, bulk modulus (B) and shear modulus (G). Note that these parameters can be related to the elastic parameters of the Elastic Modulus, E, and Poisson's ratio, ν , from the equations:

$$B = E / (3(1-2\nu))$$

$$G = E / (2(1+\nu))$$

Typical values for materials are suggested in the FLAC-3D manual and for convenience, are shown in tables 1 and 2 for soil and rock, respectively. These elastic properties are appropriate for intact rock, but not for jointed rock in large rock masses.

Approximations have been suggested for estimating field scale properties of jointed rock from laboratory tests. Goodman (1980), for example, suggests that a reduction in modulus assuming joints regularly spaced at a distance, s , can be surmised using properties from a test of the jointed properties. If a joint displacement test is run in the laboratory (a direct shear test), the shear stiffness, k_s , can be found as the slope of the shear-stress/shear-displacement curve until the joint slips. The adjusted jointed property for, say, shear modulus, G_j , becomes:

$$1/G_j = 1/G + 1/(k_s s)$$

Table 1.—Selected elastic constants (laboratory-scale) for soil (Itasca examples adapted from Das [1994]) (Note: Original ranges in table are averaged)

Material	Dry density		E		PR	K		G	
	lb/ft ³ *	lb/in ³	lb/ft ²	lb/in ²		lb/ft ²	lb/in ²	lb/ft ²	lb/in ²
Loose uniform sand	91.77	5.73	3.76E+05	2.61E+03	0.3	3.13E+05	2.18E+03	1.45E+05	1.00E+03
Dense uniform sand	114.87	7.17	1.08E+06	7.47E+03	0.375	1.43E+06	9.96E+03	3.91E+05	2.72E+03
Loose, angular-grained, silty sand	101.76	6.35							
Dense, angular-grained, silty sand	121.11	7.56			0.3				
Stiff, clay	108.00	6.74	2.09E+05	1.45E+03	0.35	2.32E+05	1.61E+03	7.74E+04	5.37E+02
Soft, clay*	83.03	5.18	5.22E+04	3.63E+02	0.2	2.90E+04	2.01E+02	2.18E+04	1.51E+02
Loess	86.15	5.38							
Soft organic clay*	44.64	2.79							
Glacial till	134.22	8.38							
Itasca example dam Foundation Soil 1	125.00	7.80	1.28E+07	8.86E+04	0.3	1.06E+07	7.38E+04	4.91E+06	3.41E+04
Itasca example dam Foundation Soil 2	125.00	7.80	1.28E+07	8.86E+04	0.3	1.06E+07	7.38E+04	4.91E+06	3.41E+04
Itasca example dam Embankment Soil 1	113.00	7.05	6.84E+06	4.75E+04	0.3	5.70E+06	3.96E+04	2.63E+06	1.83E+04
Itasca example dam Embankment Soil 2	120.00	7.49	6.84E+06	4.75E+04	0.3	5.70E+06	3.96E+04	2.63E+06	1.83E+04
Itasca example dam Dynamic Soil Properties	125.00	7.80						6.27E+06	4.35E+04

*Value was averaged from range

Table 2.—Selected elastic constants (laboratory-scale) for rock (adapted from Goodman [1980]) (Note: Original ranges in table are averaged)

Material	Dry density* (lb/ft ³)	Dry density (lb/in ³)	E (million lb/in ²)	Poisson's ratio	B (million lb/in ²)	G (million lb/in ²)
Sandstone			2.80	0.38	3.89	1.02
Siltstone			3.81	0.22	2.26	1.57
Limestone	130.47	8.15	4.13	0.29	3.28	1.61
Shale*	149.20	9.31	1.61	0.29	1.28	0.62
Marble	168.56	10.52	8.09	0.25	5.40	3.23
Granite			10.70	0.22	6.37	4.38

*Value was averaged from range

Elastic constants can also be calculated for soils, treated as an ideal elastic material. Assuming K_0 , the lateral pressure fractional proportion, for normally consolidated soils can be found by the empirical relationship:

$$K_0 = 1 - \sin N$$

where,

N = the internal angle of soil friction

For constructed backfills, K_0 (at rest) conditions may not correctly estimate the soil condition.

Poisson's ratio, ν , for drained conditions may be found as:

$$\nu = (1 - \sin N) / (2 - \sin N)$$

For fully saturated conditions, the Poisson's ratio will be just under 0.5 because the incompressible water will dominate. Samples may be tested directly in the laboratory. Using the conventional triaxial cell allows a chosen confining pressure to be applied. This procedure allows initial elastic properties, elastic properties induced by stress changes, strength values, and postfailure properties to be calculated. Although sampling of loose materials may be problematic and expensive, laboratory-tested samples allow strength and postfailure measurements to be made, which are otherwise impossible.

In situ (field) measurements can be made and used to estimate linear elastic properties. Small strain values of G can be estimated using shear wave velocities measured during cross-hole tests. The following equation is generally used to estimate G_{\max} for both static and dynamic models:

$$G_{\max} = DVs^2$$

where,

G_{\max} = maximum shear modulus

D = mass density (unit weight/g, where g is the acceleration of gravity)

V_s = measured shear wave velocity

Bulk modulus, K_{\max} , is a function of G_{\max} and Poisson's ratio and is determined using the following equation:

$$B_{\max} = G_{\max} \frac{2(1+\nu)}{3.0(1-2\nu)}$$

where,

B_{\max} = bulk modulus

ν = Poisson's ratio

Strain rate effects may be present in geotechnical materials. In such cases, the shear wave measurements may better represent a dynamic (earthquake) event. The correlation with wave velocity may not be correct for all in-situ materials. This effect needs further study.

Stress-Dependent Properties

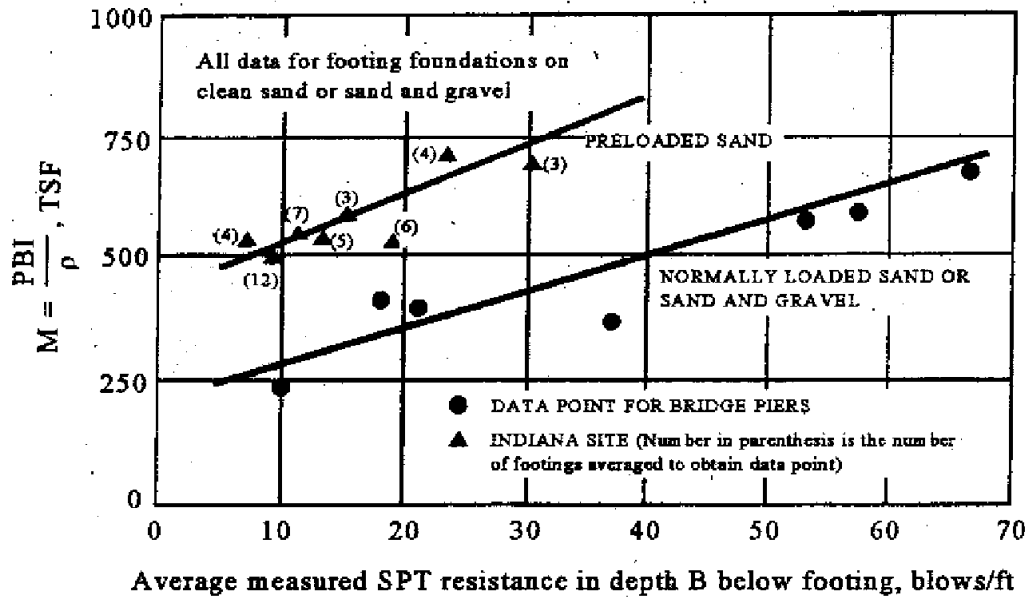
Stress-strain curves for soils are nonlinear and dependent on confining pressures. As the deviator stress ($\sigma_1 - \sigma_3$) increases, the slope of the stress-strain curve decreases. As the confining stress, σ_3 , increases, the strength of the soil and the steepness of the stress-strain curve increases. Thus, even for an ideal, homogeneous soil, the properties vary spatially because of the variation in the stress field. For this reason, the initial slope, or a secant slope, to the stress-strain curve may not properly represent the modulus value desired. An unload-reload slope from a predetermined value of stress would represent this value more accurately. For example, confining pressures representing an element of soil constructed 20 feet below the crest of a dam may be 20 lb/in². A conventional triaxial test would be run at this confining pressure and unload/reload cycles would be performed at increasing vertical stresses. Several cycles of increasing stress would be performed during the test. This approach allows the selection of modulus values other than the initial modulus. These values can be used in the Duncan-Chang Hyperbolic Material Model. This approach would also help establish the plastic offsets for a given stress state as is needed in properties noted later, or would be the correct value for use.

To aid in the selection of in-situ properties, an empirical correlation between standard penetration test (SPT) blow counts and the Modulus of Compressibility, M , is suggested by Duncan and Wong (1999), based on work from D'Appolonia (1970), as shown in figure 1. The Secant Modulus, E_s , may be estimated from M , and the sand angle of friction, N , using tabulated values as shown in table 3.

Intrinsic Strength Properties (Initiation of Failure)

The single most important determinant of large deformation magnitude is material strength. It can also be one of the more difficult properties to accurately characterize, especially at depth and in foundations with complex layering. The basic failure criterion in FLAC-3D is the Mohr-Coulomb relation. The two strength constants, c and N , are conventionally derived from laboratory triaxial tests. For simplicity, the Mohr-Coulomb line is extended into the tensile stress quadrant. The maximum value of tension is thus $c/\tan(N)$.

Typical values for materials are suggested in the FLAC3D manual and, for convenience, are tabulated in tables 4 through 6. Note that values for clayey soils depend on stress history, especially cohesion. The reported friction angles may need to be reviewed for placed materials, versus the use for natural materials.



Note : P = bearing pressure, B = footing width, I = elastic settlement influence factor, and ρ = measured settlement.

Figure 1.—Interpretation of Modulus of Compressibility from SPT data.

Table 3.—Estimating the Secant Modulus, E_s

N (degrees)	Poisson's ratio	E_s/M
55	0.15	0.94
50	0.19	0.91
45	0.23	0.87
40	0.26	0.81
35	0.30	0.75
30	0.33	0.67
25	0.37	0.58
20	0.40	0.48
15	0.43	0.37
10	0.45	0.25
5	0.48	0.13
0	0.50	0.00

Table 4.—Selected strength properties (laboratory-scale) for rock (adapted from Goodman [1980])

Material	Friction angle (degrees)	Cohesion (lb/in ²)	Tension strength (lb/in ²)
Berea sandstone	27.8	3945.03	169.69
Repetto siltstone	32.1	5032.81	
Muddy shale	14.4	5569.45	
Sioux quartzite	48.0	10,239.66	
Indiana limestone	42.0	974.65	229.16
Stone Mountain granite	51.0	7991.58	
Nevada Test Site basalt	31.0	9601.50	1899.99

Table 5.—Selected strength properties (drained, laboratory-scale) for soils (adapted from Ortiz et al. [1986])

Material	Cohesion		Friction angle (degrees)	
	lb/ft ³	lb/in ²	Peak	Residual
Gravel			34	32
Sandy gravel with few fines			35	32
Sandy gravel with silty or clayey fines	21	0.15	35	32
Mixture of gravel and sand with fines	62	0.44	28	22
Uniform sand—fine			32	30
Uniform sand—coarse			34	30
Well-graded sand			33	32
Low-plasticity silt	42	0.29	28	25
Medium to high plasticity silt	62	0.44	25	22
Low plasticity clay	125	0.87	24	20
Medium plasticity clay	167	1.16	20	10
High plasticity clay	208	1.45	17	6
Organic silt or clay	146	1.02	20	15

Table 6.—Selected other strength properties

Material	Cohesion		Friction angle (°)	
	lb/ft ³	lb/in ²	Peak	Residual
Itasca example dam Foundation Soil 1	83.5	0.58	0.58	40
Itasca example dam Foundation Soil 2	160	1.11	1.11	40
Itasca example dam Embankment Soil 1	120	0.83	0.83	35
Itasca example dam Embankment Soil 2	120	0.83	0.83	35
USBR <i>Design of Small Dams</i> —GP	70.8	0.49	5.9	41.4
USBR <i>Design of Small Dams</i> —GM	160.8	1.12	13.4	34
USBR <i>Design of Small Dams</i> —GC	122.4	0.85	10.2	27.5
USBR <i>Design of Small Dams</i> —SP	66	0.46	5.5	37.4
USBR <i>Design of Small Dams</i> —SM	79.2	0.55	6.6	33.6
USBR <i>Design of Small Dams</i> —SC	60	0.42	5	33.9
USBR <i>Design of Small Dams</i> —ML	43.2	0.30	3.6	34
USBR <i>Design of Small Dams</i> —CL	123.6	0.86	10.3	25.1
USBR <i>Design of Small Dams</i> —CH	138	0.96	11.5	16.8

In situ (field) measurements can be made. Material strengths are usually derived from empirical correlations with SPT or cone penetration test (CPT) data (Robertson and Campanella, 1983). Interpretation of SPT data can be quite complex, especially when the test conditions differ from standard conditions used to develop the correlations. The results of the test are strongly influenced by the presence of gravel, the SPT hammer efficiency, the depth of testing, and many other factors. An advantage to using SPT, over other methods such as the CPT, is that a sample can be taken allowing material classification and testing.

Reclamation does not use the CPT as often as the SPT, but it is faster and produces a nearly continuous record of penetration resistance. The CPT is a good choice for determining stratigraphy over a large area although it does not produce samples for classification or testing as does the SPT.

The Becker hammer test (BPT) can be used in soils that are too gravelly to produce meaningful CPT or SPT data (Harder and Seed, 1986). Interpretation of BPT data is more uncertain than for the SPT since there is a smaller body of historical data supporting BP correlations with strength and liquefaction

resistance. With more use and analysis, the BPT may become a more common method of in situ strength determination.

Postfailure Properties

The response of a material after failure has initiated can be an important factor in engineering design. If postfailure behavior is to be estimated with the analysis, postfailure properties must be simulated in the model. This is accomplished by using all of the following properties, each of which defines postfailure responses:

1. Shear dilatancy
2. Shear hardening/softening
3. Tensile softening

Shear Dilatancy

Usually determined from triaxial tests or shear box tests, shear dilatancy describes the slope of a line of volumetric strain increase versus axial strain (see fig. 2).

The value is typically less than N . The FLAC-3D manual suggests the following typical values:

<u>Typical values for dilation angle (Vermeer and deBorst [1984])</u>	
Dense sand	15°
Loose sand	$< 10^\circ$
Normally consolidated clay	0°
Granulated and intact marble	$12^\circ - 20^\circ$
Concrete	12°

Note that dilatancy effects are appropriate up to a limited strain or displacement amount. Beyond this value, the kinematic effects, not the material dilatancy, control the resistance to displacement.

Shear Hardening/Softening

The initiation of material hardening or softening is a gradual process once plastic yield begins. This leads to a degradation in strength. Shear hardening and softening are simulated by making Mohr-Coulomb properties (cohesion, friction, and dilation angle) to be functions of plastic strain.

Hardening and softening parameters must be calibrated for each specific analysis, and the values are generally back-calculated from results of laboratory tests.

Numerical testing conditions can influence the model response for shear hardening/softening behavior. The rate of loading can introduce inertial effects. The results are also grid-dependent.; rebound effects may need to be absorbed by several elements, and element size may need to be adjusted in areas of softening and tension behavior.

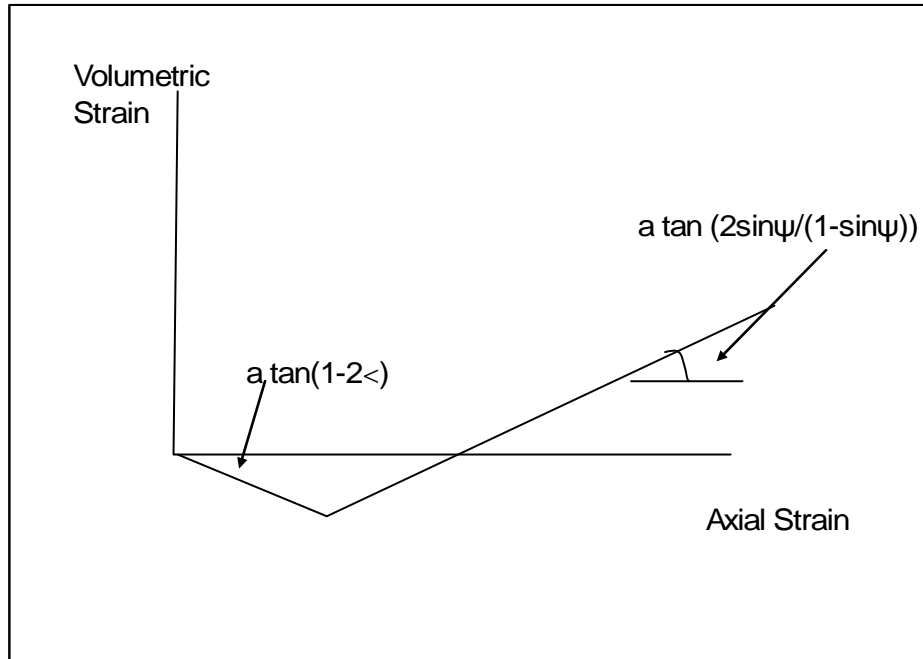


Figure 2.—Definition of shear dilatancy.

Tensile Softening

At the initiation of tensile failure, the tensile strength of a material will generally drop to zero. The rate at which tension strength drops, or tensile softening occurs, is controlled by the plastic strain in FLAC-3D. A simple tension test demonstrates the tensile-softening behavior.

Large Strain Properties in FLAC

At large strains, geologic materials become softer as K and G are reduced. These values may be found directly through sampling and testing. At high strain levels (between 2% and 10%) laboratory data in terms of modulus reduction and damping are scarce. These data are generated using either a Cyclic Triaxial Test or a Resonant Column test. In practice, these curves are usually extrapolated for use in site response analysis, but may be without a sound basis (Makdisi and Wang, 2004). Methods to estimate the properties are discussed below; however, site-specific values need to be used for all but preliminary studies of critical structures.

Data are available in the literature for these properties. A recent study (Roblee and Chiou, 2004) suggests, based on 154 tests from 28 different sites, that the values may be estimated through the classification properties of gradation and plasticity. Typical values from this study are shown in table 7, with associated graphs shown in figures 3 through 5.

Table 7.—Shear modulus and damping factors for soil classifications (Roblee and Chiou, 2004)

Depth (meters)		Shear strain (%)	1-PCA, Primarily coarse		2-FML, Fine grained low plasticity		3-FMH, Fine grained high plasticity	
Min	Max		G/G _{max}	D (%)	G/G _{max}	D (%)	G/G _{max}	D (%)
0	10	1.00E-04	0.993	1.34	0.997	1.32	0.999	1.32
		3.16E-04	0.981	1.43	0.991	1.37	0.996	1.35
		1.00E-03	0.950	1.71	0.974	1.53	0.987	1.45
		3.16E-03	0.877	2.53	0.931	2.02	0.962	1.78
		1.00E-02	0.729	4.64	0.827	3.38	0.891	2.75
		3.16E-02	0.503	8.65	0.630	6.56	0.725	5.30
		1.00E-01	0.275	13.39	0.376	11.67	0.460	10.42
		3.16E-01	0.125	16.97	0.176	16.72	0.216	17.00
		1.00E+00	0.051	18.80	0.071	19.86	0.082	21.95
		3.16E+00	0.020	19.04	0.026	20.83	0.028	23.84
10	20	1.00E-04	0.994	1.18	0.997	1.17	0.999	1.16
		3.16E-04	0.985	1.25	0.992	1.22	0.996	1.19
		1.00E-03	0.961	1.45	0.977	1.35	0.989	1.29
		3.16E-03	0.904	2.07	0.938	1.78	0.966	1.57
		1.00E-02	0.779	3.72	0.844	3.00	0.903	2.43
		3.16E-02	0.570	7.23	0.657	5.94	0.750	4.74
		1.00E-01	0.332	11.98	0.404	10.89	0.493	9.55
		3.16E-01	0.158	15.99	0.194	16.07	0.239	16.12
		1.00E+00	0.066	18.32	0.079	19.47	0.092	21.38
		3.16E+00	0.026	18.96	0.029	20.66	0.032	23.61
20	40	1.00E-04	0.996	1.04	0.997	1.04	0.999	1.03
		3.16E-04	0.989	1.09	0.993	1.08	0.997	1.06
		1.00E-03	0.971	1.24	0.980	1.20	0.990	1.14
		3.16E-03	0.925	1.69	0.945	1.58	0.970	1.39
		1.00E-02	0.823	2.96	0.858	2.67	0.914	2.15
		3.16E-02	0.636	5.90	0.682	5.36	0.774	4.22
		1.00E-01	0.396	10.50	0.433	10.15	0.526	8.73
		3.16E-01	0.198	14.88	0.213	15.42	0.264	15.23
		1.00E+00	0.085	17.71	0.088	19.07	0.104	20.79
		3.16E+00	0.034	18.80	0.033	20.49	0.036	23.37
40	80	1.00E-04	0.997	0.92	0.998	0.92	0.999	0.91
		3.16E-04	0.991	0.95	0.994	0.95	0.997	0.93
		1.00E-03	0.978	1.06	0.982	1.06	0.991	1.00
		3.16E-03	0.943	1.39	0.951	1.39	0.974	1.23
		1.00E-02	0.860	2.34	0.873	2.35	0.923	1.90
		3.16E-02	0.699	4.73	0.709	4.80	0.795	3.77
		1.00E-01	0.466	8.98	0.463	9.37	0.556	7.98
		3.16E-01	0.247	13.63	0.235	14.72	0.289	14.38
		1.00E+00	0.110	16.96	0.098	18.63	0.116	20.19
		3.16E+00	0.044	18.53	0.037	20.31	0.041	23.11
80	160	1.00E-04	0.998	0.81	0.998	0.81	0.999	0.81
		3.16E-04	0.994	0.83	0.996	0.83	0.997	0.83
		1.00E-03	0.984	0.90	0.986	0.90	0.992	0.90
		3.16E-03	0.959	1.12	0.966	1.12	0.974	1.12
		1.00E-02	0.898	1.78	0.910	1.78	0.925	1.77
		3.16E-02	0.769	3.53	0.781	3.56	0.800	3.59
		1.00E-01	0.556	7.14	0.559	7.37	0.564	7.73
		3.16E-01	0.320	11.91	0.310	12.72	0.295	14.09
		1.00E+00	0.150	15.83	0.138	17.34	0.119	19.96
		3.16E+00	0.062	18.05	0.054	19.84	0.042	22.97
160 +		1.00E-04	0.998	0.71	0.999	0.71	0.999	0.71
		3.16E-04	0.996	0.72	0.997	0.72	0.998	0.72
		1.00E-03	0.989	0.77	0.992	0.77	0.994	0.77
		3.16E-03	0.971	0.91	0.977	0.91	0.983	0.91
		1.00E-02	0.927	1.35	0.937	1.35	0.950	1.34
		3.16E-02	0.827	2.58	0.840	2.60	0.859	2.60
		1.00E-01	0.643	5.46	0.651	5.58	0.664	5.76
		3.16E-01	0.404	10.03	0.398	10.58	0.390	11.48
		1.00E+00	0.203	14.45	0.190	15.73	0.171	17.93
		3.16E+00	0.087	17.33	0.077	19.07	0.063	22.12

Computer Material Models for Soils Using FLAC and DYNA

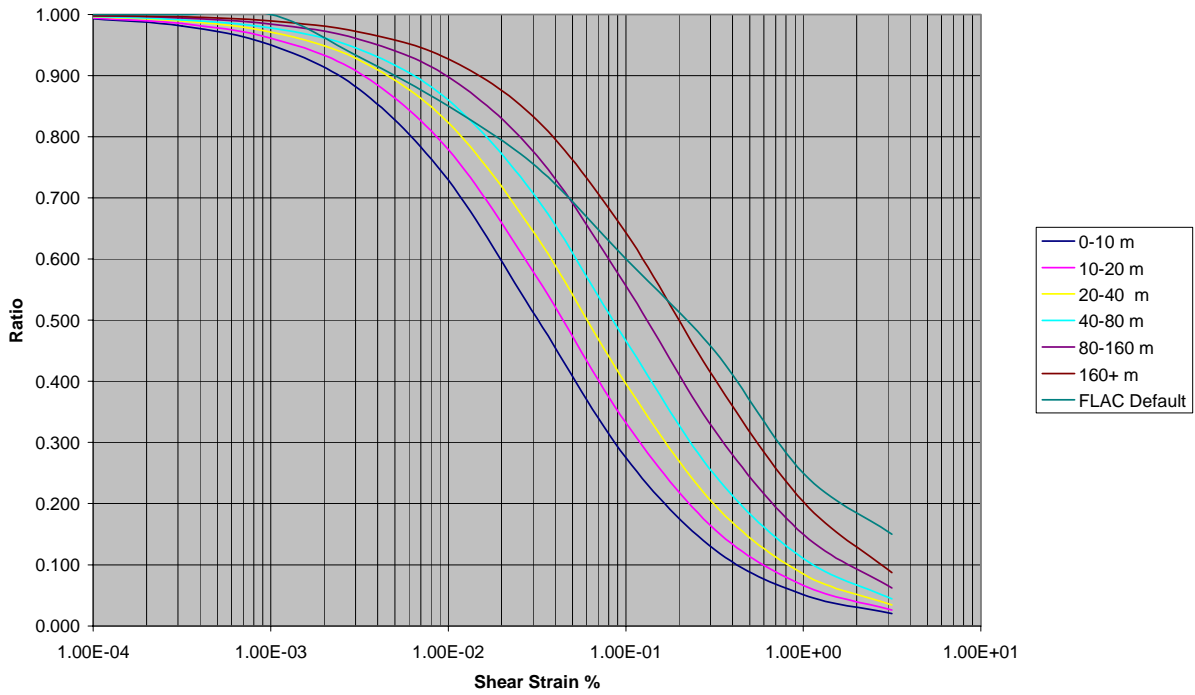


Figure 3.— G/G_{max} at increasing depths for primarily coarse materials and all plasticity values.

G/Gmax Fine Grained High Plasticity

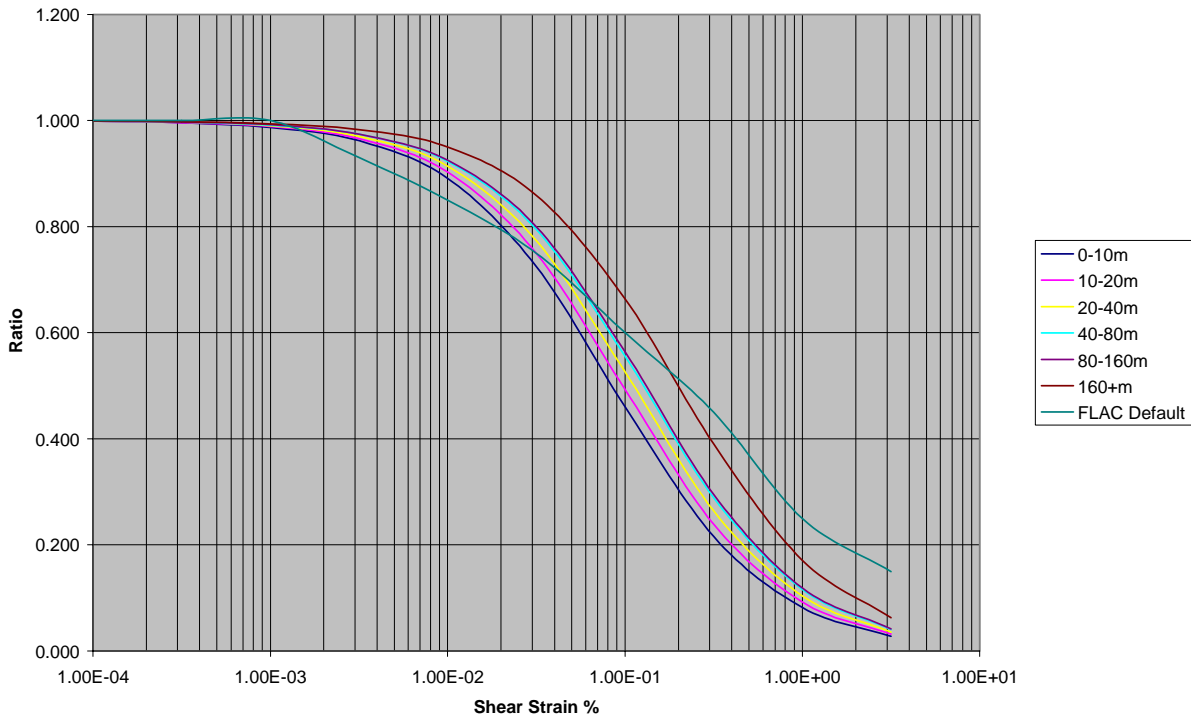


Figure 4.— G/G_{max} at increasing depths for fine grained, high plasticity materials.

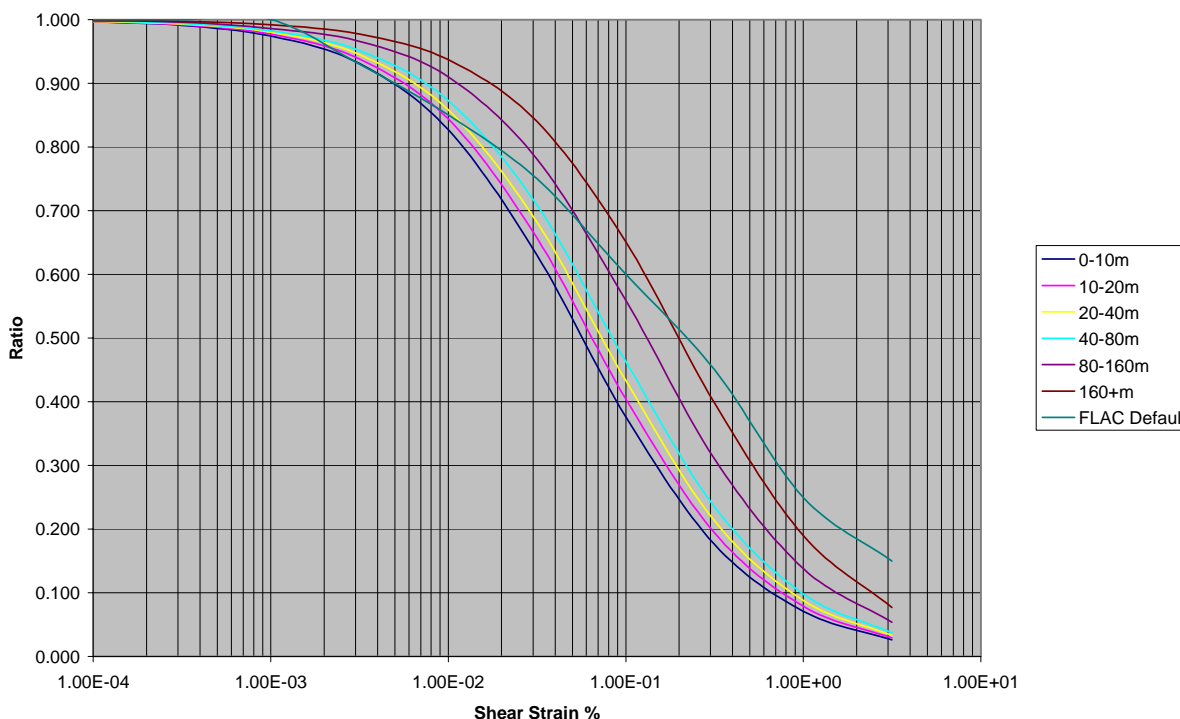


Figure 5.— G/G_{\max} at increasing depths for fine grained materials with $PI < 15\%$.

Empirical estimates of the reduction factor, G/G_{\max} , can be made using the computer program SHAKE (Idriss and Sun, 1991) by employing a one-dimensional analyses of a soil column having the same stratigraphy, shear wave velocities, unit weights, and applied acceleration time history as those employed in FLAC. The SHAKE program computes the response of a semi-infinite horizontally layered soil deposit overlying a uniform half-space subjected to vertically propagating shear waves. It accounts for modifications to the input wave due to propagation through the upper soil layers to the free ground surface. In SHAKE, the analysis is done in the frequency domain and, therefore, for any set of properties, is a linear analysis. An iterative procedure is used to account for the nonlinear behavior of the soils to obtain values for modulus and damping that are compatible with the equivalent uniform strain induced in each sub-layer. At the beginning of the analysis, a shear modulus, damping factor, and unit weight are assigned to each sublayer of the soil. Shear strains induced in each sublayer are calculated during the time history analysis. Using applicable relationships between (1) shear modulus and strain and (2) damping ratio and strain, the shear modulus and damping ratio of each sublayer are modified. The analysis is repeated until strain compatible properties are obtained. Accelerations from each sublayer of soil are also available.

Liquefiable Strengths

Most often, liquefied shear strengths are determined using empirical correlations to the SPT (Seed and Harder, 1990). A typical field investigation program will generate numerous SPT data for use in analysis. For each zone of liquefiable material, a representative penetration resistance is chosen on which to base the strength used for analysis. This is sometimes assumed to be the mean of the lowest penetration values from each profile within the area of potential failure. The 25th or 33rd percentile of all the relevant data is also sometimes used, but one must evaluate whether the spatial distribution of the lowest penetration values makes this appropriate. If a distinct weak layer exists, data from that layer need to be considered separately from the surrounding material when selecting the strength.

Cone penetration test data can be used to estimate an equivalent $(N_1)_{60}$ -CS, but combining two correlations makes the resulting strength estimate even more uncertain than with the single SPT correlation. Several different laboratory shear testing procedures have been proposed for estimating the postliquefaction residual undrained shear strength. All involve recovery of undisturbed samples of the material in question, and undrained cyclic or monotonic shear testing. No sample is truly undisturbed, and undrained shear strength is very sensitive to minor changes in density. Laboratory shear tests on small volumes of material cannot account for mass soil behaviors such as void redistribution, and strains in common laboratory devices are limited to values far below those that occur in flow slides. For these reasons, laboratory procedures for assessing the postliquefaction, undrained shear strength for a particular site have not received full acceptance within the profession.

Under the current state of the art, postliquefaction strength of soils is not fully understood. The data supporting SPT strength correlations are few and of variable quality. Because both laboratory test measurements and correlations with in situ properties have serious drawbacks, neither approach can be considered a definitive indication of the available strength. The uncertainty in strength estimates must be acknowledged, and sensitivity to variations in strength must be evaluated.

Parameter and Testing Requirements for FLAC-3D

Table 8 summarizes FLAC properties and recommended tests.

Note that to find plastic strain at a given stress level, an unload-reload test needs to be conducted during a stress-strain test. By doing subsequent tests until failure, a final plastic strain can be estimated for the c and ϕ values calculated from the Mohr-Coulomb failure circles. Failure angles should be measured following failure for each test so that a c and ϕ can also be estimated individually for the tests. This construction is shown in figure 6.

Table 8.—FLAC properties and recommended tests

Stress state	Parameter	Recommended test	Needed data
Elastic	K, bulk modulus G, shear modulus	Conventional triaxial with volumetric measurements Direct shear test	K: stress vs. volumetric strain G: shear stress vs. shear strain Alternate data: E: Axial stress vs. axial strain PR: Lateral strain vs. longitudinal strain
Failure	Mohr-Coulomb C, cohesion Phi, ϕ	Conventional triaxial Alternate: Direct shear test	Shear stress vs. normal stress for at least 3 confining pressures Shear stress vs. normal stress for at least 3 normal stresses
Postfailure			
a. Shear dilatancy	Dilation angle		Volumetric strain vs. axial strain
b. Shear hardening/softening	C Phi, and Dilation angle vs. plastic strain	Conventional triaxial with unload/reload	Parameter vs. plastic strain
c. Tension softening		Uniaxial tension test	Plastic strain vs. tensile strength
Large strains			
Modulus vs. shear strain (see also Damping section later)	Modulus at various shear strains	Cyclic triaxial test or resonant column test	Ratio of modulus vs. shear strain graph

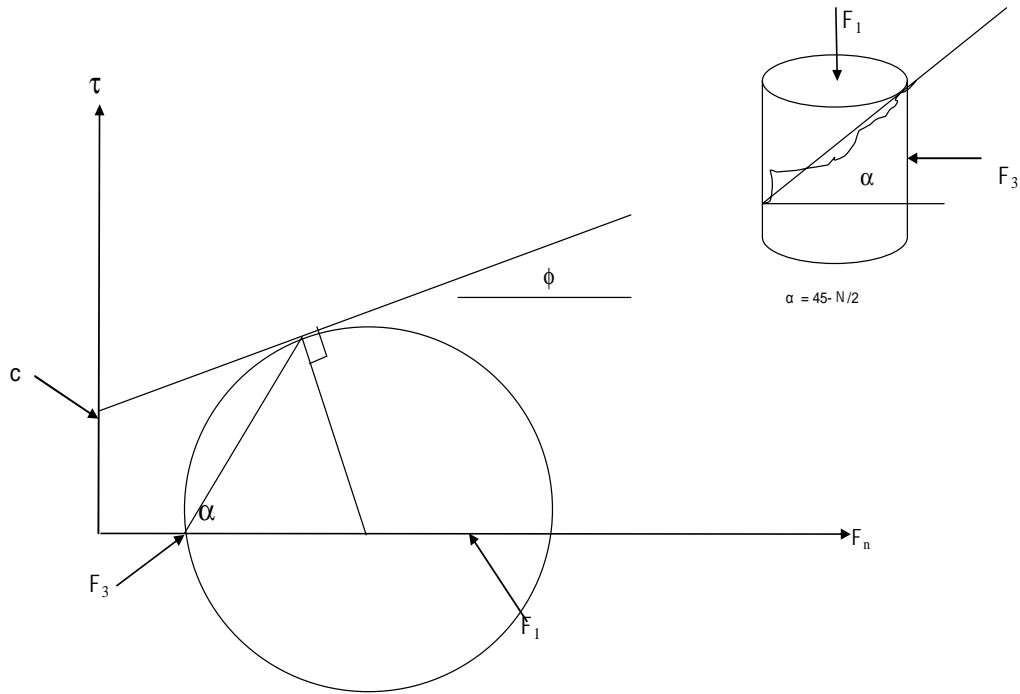


Figure 6.—Finding c and ϕ from a measured angle, α .

Calculation of Dynamic Pore Pressures

This information is from the *FLAC-3D Manual*, “Optional Features—Dynamic Pore-Pressure Generation.”

Coupled dynamic-groundwater flow calculations can be performed using *FLAC-3D*. By default, the pore fluid simply responds to changes in pore volume caused by the mechanical dynamic loading. The *average* pore pressure remains essentially constant in the analysis.

It is known that pore pressure may build up considerably in some sands during cyclic shear loading. Eventually, this process may lead to liquefaction when the effective stress approaches zero. There are many different models that attempt to account for pore pressure buildup, but they often do it in an ill-defined manner because they refer to specific laboratory tests. In a computer simulation, there will be arbitrary stress and strain paths. Consequently, an adequate model must be robust and general, with a formulation that is not couched in terms that apply only to specific tests. We chose here a model that is simple, but that accounts for the basic physical process.

Finn and Byrne Models (Byrne, 1991)

This section is directly from the *FLAC-3D Manual*, “Optional Features”:

In reality, pore pressure buildup is a *secondary* effect, although many people seem to think it is the primary response to cyclic loading. The primary effect is the irrecoverable volume contraction of the matrix of grains when a sample is taken through a complete strain cycle when the confining stress is held constant. Since it is grain rearrangement rather than grain volume change that takes place, the volume of the void space decreases under constant confining stress. If the voids are filled with fluid, then the pressure of the fluid increases, and the effective stress acting on the grain matrix decreases. Note that pore pressures would not increase if the test were done at constant volume; it is the transfer of externally applied pressure from grains to fluid that accounts for the fluid-pressure increase.

Martin et al. (1975) defined this mechanism, also noting that the relation between irrecoverable volume-strain and cyclic shear-strain amplitude is independent of confining stress. They supply the following empirical equation that relates the increment of volume decrease, ϵ_{vd} , to the cyclic shear-strain amplitude, γ , where γ is presumed to be the “engineering” shear strain:

$$\epsilon_{vd} = C_1((\gamma - C_2)^2 + C_3) / (C_4 + \gamma)$$

where C_1 , C_2 , C_3 , and C_4 are constants.

Note that the equation involves the accumulated irrecoverable volume strain, ϵ_{vd} , in such a way that the increment in volume strain decreases as volume strain is accumulated. Presumably, ϵ_{vd} should be zero if γ is zero; this implies that the constants are related as follows: $C_1 C_2 C_4 = C_3$. Martin, et al. (1975) then go on to compute the change in pore pressure, by assuming certain moduli and boundary conditions (which are not clearly defined). We do not need to do this. Provided we correctly account for irreversible volume change in the constitutive law, FLAC-3D will take care of the other effects.

An alternative, and simpler formula is proposed by Byrne (1991):

$$\epsilon_{vd} / \gamma = C_1 \exp(-C_2(\gamma / C_3))$$

where C_1 and C_2 are constants with different interpretations from those of the previous equation. In many cases $C_2 = 0.4/C_1$ so this equation involves only one independent constant; however, both C_1 and C_2 have been retained for generality. In addition, a third parameter, C_3 , sets the threshold shear strain (i.e., the limiting shear strain amplitude below which volumetric strain is not produced).

FLAC-3D contains a built-in constitutive model (named the “Finn model”) that incorporates these equations into the standard Mohr-Coulomb plasticity model—it can be modified by the user as required. The use of the first or second equation can be selected by setting parameter **ff_switch** = 0 or 1, respectively. As it stands, the model captures the basic mechanism that can lead to liquefaction in sand. In addition to the usual parameters (friction, moduli, etc.) the model needs four constants for the first equation, or three constants for the second equation. For the

first equation, Martin et al. (1975) describe how these may be determined from a *drained* cyclic test. Alternatively, one may imagine using some trial values to model an undrained test with FLAC-3D and compare the results with a corresponding laboratory test; the constants could then be adjusted to obtain a better match. For the second equation, Byrne (1991) notes that the constant, C_1 , can be derived from relative densities, D_r , as follows:

$$C_1 = 7600(D_r)^{-2.5}$$

Further, using an empirical relation between D_r and the normalized penetration test values, $(N_1)_{60}$:

$$D_r = 15(N_1)_{60}^{1/2}$$

Then,

$$C_1 = 8.7(N_1)_{60}^{-1.25}$$

C_2 is then calculated from $C_2 = 0.4/C_1$ in this case. Refer to Byrne (1991) for more details.

In the Finn model, there is logic to detect a strain reversal in the general case. (Author's note: Strain reversal is a change in sign in the strain condition). In Martin et al. (1975) (and most other papers on this topic), the notion of a strain reversal is clear because they consider one-dimensional measures of strain. In a three-dimensional analysis, however, there are at least six components of the strain tensor. A threshold is set to monitor strain reversals (to prevent reversal logic being triggered again on transients that immediately follow a reversal) (Author's note: The intent is to not let the reversals in 1 of the 6 directions revert back and forth in sign, causing iterations on each occurrence). This threshold number of time steps is controlled by the property named **ff_latency**, which is set to 50.0 in example runs in the manual.

The Finn model is implemented in FLAC-3D with the **MODEL** command, i.e., **MODEL Finn**. The code must be configured for dynamic analysis (**CONFIG dynamic**) to apply the model. As with the other built-in models, the properties are assigned with the **PROPERTY** command. The following keywords are used to assign properties for the Finn model:

bulk	bulk modulus
cohesion	cohesion
dilation	dilation angle in degrees
ff_c1	constant C_1 in either pore pressure equation
ff_c2	constant C_2 in either pore pressure equation
ff_c3	constant C_3 in equation 1 or threshold shear strain in equation 2
ff_c4	constant C_4 in equation 1
ff_latency	minimum number of time steps between reversals
ff_switch	0 for equation 1, 1 for equation 2
friction	friction angle in degrees
shear	shear modulus
tension	tension limit

The default values for these properties are zero.

The user should verify that the algorithm is appropriate before applying it to real cases. In particular, the number of “cycles” detected depends strongly on the relative magnitude of horizontal and vertical motion. Hence, the rate of buildup of pore pressures will also be sensitive to this ratio. It may be more practical to consider just the shear components of strain for something like a dam, which is wide compared to its height. Ultimately, we need better experimental data for volume changes during complicated loading paths; the model could then be revised accordingly. One effect that has been shown to be very important is the effect of rotation of principal axes: volume compaction may occur even though the magnitude of deviatoric strain (or stress) is kept constant. Such rotations of axes occur frequently in earthquake situations. Another effect that is not incorporated in the Finn model is that of the modulus increase induced by compaction—it is known that sand becomes stiffer elastically when compaction occurs by cyclic loading.

User-Supplied Materials in FLAC

Hyperbolic Model

FLAC allows users to supply their own material models through the input files, and using the FISH programming language. Thus, many variations are possible for material models. A model commonly discussed is the Hyperbolic Model (Duncan and Chang, 1970) or variations from this original model.

The Hyperbolic Model recognizes that stress-strain graphs have the general shape of a hyperbola. The values that control the shape of the hyperbola are the initial Modulus of Elasticity, E_i , and the deviatoric stress ($F_1 - F_3$). The curves at failure may be related the Mohr Coulomb Failure Criterion to incorporate a method to calculate the initiation of failure and stress-strain behavior following behavior. The calculation method for these two principles is described in the following paragraphs.

Triaxial test results are needed at varying confining pressures. These tests can be used to find relationships for effective stress analysis using data from drained triaxial tests, or for total stress analysis using data from Unconsolidated-Undrained triaxial tests. Stress-strain data from Consolidated-Undrained triaxial tests cannot be applied directly but can be used if interpreted logically. Data from the tests are plotted on a log-log scale with the confining pressure, F_3 , divided by the atmospheric pressure, P_a , (in appropriate units) on the x-axis and the initial modulus divided by the atmospheric pressure on the y-axis. The data represented in this format generally plot as a straight line, or can be fitted to a straight line. The hyperbolic constant, K , is found as the y-axis intercept on this graph at $F_3/P_a = 1$. The hyperbolic constant, n , is found as the value that best fits the straight line through the data, satisfying the equation:

$$E_i/P_a = K(F_3/P_a)^n$$

The failure ratio, R_f , is found as the ratio of the compressive strength $(F_1 - F_3)_f$ divided by the hyperbolic asymptote, $(F_1 - F_3)_{ult}$. Variation of compressive strength with confining pressure is represented by the Mohr-Coulomb strength equation, which can be expressed in the form:

$$(F_1 - F_3)_f = (2c \cos N + 2 F_3 \sin N)/(1 - \sin N)$$

where c is the cohesion intercept (in appropriate stress units) and N is the angle of internal friction found using standard tests at a given confining pressure, F_3 . Note that these parameters may be found using a direct shear test or conventional triaxial tests.

These parameters can then be used to calculate the tangent Modulus of Elasticity for any given stress state using the equation:

$$E_t = [1 - (R_f(1 - \sin N)(F_1 - F_3)/(2c \cos N + 2F_3 \sin N))]^2 K P_a (F_3/P_a)^n$$

A Modulus of Elasticity for unloading and reloading conditions can be defined separately using test data from unload-reload cycles and fitting in the manner described above to find the hyperbolic constants:

$$E_{ur}/P_a = K_{ur} (F_3/P_a)^n$$

In addition, a variation of the friction angle can be found using a constant, ΔN , which is the decrease in friction angle for a tenfold increase in F_3 .

Typical values for hyperbolic parameters have been published (Duncan and Wong, 1999) and are shown in table 9. As noted previously, there is a difference in properties based on relative compaction percentage (placed materials).

Other Hyperbolic Variations

As noted in the section describing *Linear Elastic Properties*, the elastic properties of B , bulk modulus, and G , shear modulus, may also be used to express linear properties; in a hyperbolic form, these would be shown as:

$$B_t = K_B P_a (F_3/P_a)^{be}$$

$$G_t = K_G P_a (F_3/P_a)^{ge}$$

And the constants would be found in a similar manner as described before while considering that bulk modulus is found as the slope of the Stress-Volumetric Strain curve and G is the slope of the Shear Stress-Shear Strain graph.

Table 9—Typical hyperbolic constants (Duncan and Wong, 1999)

Unified classification	Relative density, D_r (%)	Relative compaction (%)	Grain shape	Dry density (lb/ft ³)	N) N	c (lb/ft ²)	K	K_{ur}	n	R_f
GW-SW	80-100	100	Rounded	110-130	46-52	7	500-1000	1.5K	0.5	0.65	
	80-100	100	Angular	110-130	46-52	9	300-600	1.5K	0.5	0.65	
	40-60	90	Rounded	100-120	42-48	4	300-600	2.0K	0.5	0.70	
	40-60	90	Angular	100-120	42-48	6	200-400	2.0K	0.5	0.70	
GP-SP	80-100	100	Rounded	100-140	42-48	5	500-1500	1.5K	0.4	0.80	
	80-100	100	Angular	100-140	42-48	10	300-600	1.5K	0.4	0.80	
	40-60	90	Rounded	90-125	32-38	2	300-600	2.0K	0.7	0.85	
	40-60	90	Angular	90-125	32-38	4	200-400	2.0K	0.7	0.85	
SM	100	100		95-125	35-40	7	300-600	1.6K	0.6	0.70	
	90	90		85-115	30-35	2	200-400	1.6K	0.6	0.70	
SM-SC	100	100		100-130	30-35		600-2000	2.0K	0.3	0.70	
	90	90		90-120	30-35		200-600	2.0K	0.3	0.70	
ML	100	100		100-120	35-40	7	300-600	1.6K	0.4	0.75	
	90	90		90-110	30-35	2	200-400	1.6K	0.4	0.75	
CL	100	100		100-120	27-32		400-1200	2.0K	0.5	0.50	
	90	90		90-110	27-32		100-300	2.0K	0.5	0.50	

Byrne Model

A further modification of the hyperbolic model was suggested and used for comparison of lab and centrifuge data (Puebla, Byrne, and Phillips, 1997). An approach similar to Duncan and Chang's (1970) was adopted but was modified in the following approaches: (1) the Shear Modulus, Bulk Modulus form is used with a mean confining stress rather than confining stress, (2) only the plastic component of shear strain is assumed to follow the hyperbolic formulation, and (3) the plastic shear strain is controlled by a stress ratio, rather than the shear stress only.

The elastic, hyperbolic relation for this model uses the mean stress, p' , as $(F_1' + F_3')/2$, where the stresses are the effective major principal stress and effective minor principle stress, respectively. The plastic volumetric strain increment is obtained by a plastic flow rule that incorporates the dilation angle, Q . This value can be found in conjunction with the developed friction angle, N_d as:

$$\sin Q = (\sin N_{cv} - \sin N_d)$$

where,

N_{cv} = the constant volume friction angle

The stress ratio for this formulation, denoted O_d , is found as the ratio of the deviator, $q = (F_1' - F_3')/2$, and the mean stress:

$$O_d = (q/p) = \sin N_d$$

Likewise, the failure ratio in this formulation uses the stress ratios:

$$R_f = O_f / O_{ult}$$

where O_{ult} is the ultimate strength from the best fit of hyperbola. This value generally ranges from 0.5 to 1.0.

For the undrained behavior of the soil, this formulation uses a change in pore pressure that is related to the fluid bulk modulus, B_f , and the soil porosity, n :

$$\Delta u = (B_f / n) \Delta \epsilon_v^f$$

where the strain component is the equivalent fluid volumetric strain.

Results using this model predicted displacements and pore pressures that were in reasonable agreement with a measured field event.

Strain Rate Effects

FLAC-3D does not incorporate a method to account for changes in material properties caused by high strain rates calculated during the analysis. Properties tested or adjusted for high strain rates could be used. The effect of strain rate on soils was evaluated with a state-of-the art literature search. Virtually no literature was found; this as an area for further research.

Recommendations for FLAC-3D Use

The standard material model in FLAC-3D can be successfully used for analyses. As a minimum, the elastic parameters need to be used: B , Bulk Modulus, G , Shear Modulus, and Poisson's Ratio, and the initiation of failure parameters c , cohesion, and N , angle of friction (in total stress, or effective stress as appropriate). These analyses will indicate areas of potential problems. If more sophisticated analyses, such as large deformations or liquefaction, are desired, additional postfailure parameters need to also be included that are measured for the case being modeled, or at least be selected from reference values and be deemed appropriate for the case being modeled. These include shear dilatancy angle for materials that can dilate during shearing, shear hardening/softening for materials that can harden or soften during shear strain, and tension softening for materials that can lose tension strength during shearing.

As FLAC-3D allows user-supplied models, models such as the hyperbolic model can be used by knowledgeable users with appropriate parameters..

LS-DYNA

LS-DYNA (commercial version of DYNA) is a nonlinear explicit computer code with movable mesh solution having models numbered from 1 through 196. A convenient table in the manual suggests the intended purpose for the written models and their overall capability. For the convenience of the reader, this table is abstracted here as table 10 for all models intended for soil/geologic or concrete materials.

As can be seen from the table, Group 3 includes postfailure modeling and strain rate effects, Group 2 includes postfailure modeling but NOT strain rate effects, and Group 1 includes NO postfailure modeling and NO strain rate effects. Group 3, therefore, contains the candidate models for nonlinear dynamic modeling, and Groups 2 and 3 contain candidate models for nonlinear static modeling.

The written abstracts for the models are repeated below from the manual.

Table 10.—LS-DYNA/DYNA possible soil models

Code	Model #	Name	Purpose	Failure?	Strain rate?
Group 1					
LS-DYNA(DYNA)	5(5)	Soil/Foam	Foam/Soil	N	N
LS-DYNA(DYNA)	25(25)	Inviscid Geologic cap	Soil	N	N
LS-DYNA	192	Soil Brick	General	N	N
LS-DYNA	193	Drucker-Prager	General	N	N
Group 2					
LS-DYNA	14(14)	Soil/Foam w/Failure	Foam/Soil	Y	N
LS-DYNA	78	Soil Concrete	Soil	Y	N
LS-DYNA	79	Elasto-Perfectly Plastic Soil	Soil	Y	N
Group 3					
LS-DYNA(DYNA)	16(16)	Pseudo Geological Model	Soil/Concrete	Y	Y
LS-DYNA(DYNA)	26(26)	Honeycomb	Foam/Soil	Y	Y
LS-DYNA	72(45)	Concrete Damage	Soil/Concrete	Y	Y
LS-DYNA(DYNA)	96(36)	Brittle damage	?	Y	Y

LS-DYNA Soil Material Models

Group 1 Models

#5, Soil and Foam

This is a very simple model and works in some ways like a fluid. It should be used only in situations when soils and foams are confined within a structure or when geometric boundaries are present

#25, Geologic Cap

This material model can be used for geomechanical problems or for materials such as concrete. The model includes a failure surface with plastic behavior limited by a cap surface. In this model, the two-invariant cap theory is extended to include nonlinear kinematic hardening. The cap surface may be expanded based on the plastic volumetric strain. Major advantages of this model over other classical pressure-dependent plasticity models are the ability to control the amount of dilatency produced under shear loading and the ability to model plastic compaction.

#192, Soil Brick

This material enables clay type soil materials to be modeled accurately. The stress history of the soil is calculated prior to the initialization of the model.

#193, Drucker-Prager

This model enables soil to be modeled using familiar geotechnical parameters (e.g., angle of friction). The modified Drucker-Prager yield surface is used in this material model, enabling the shape of the surface to be distorted into a more realistic definition for soils.

Group 2 Models**#14, Soil and Foam w/ Failure**

This input model is the same as Model #5; however, when the three dimensional pressure reaches the failure pressure, the element loses its ability to carry tension. It should be used in situations when soils and foams are confined within a structure or when geometric boundaries are present.

#78, Soil Concrete

This model permits concrete and soil to be efficiently modeled. Curves are used to define pressure versus volumetric strain, yield versus pressure, and yield stress versus plastic strain.

#79, Elasto-Perfectly Plastic Soil

This model is a nested surface model with five superimposed layers of elasto-perfectly plastic material, each with its own elastic moduli and yield values. Nested surface models give hysteric behavior.

Group 3 Models**#16, Pseudo Geologic**

This model has been used to analyze buried steel reinforced concrete structures subjected to impulsive loadings.

This model can be used in two major modes—a simple tabular pressure-dependent yield surface, and a potentially complex model featuring two yield-versus-pressure functions with the means from migrating from one curve to the other. For both modes, load curve N1 is taken to be a strain rate multiplier for the yield strength.

#26, Honeycomb

The major use of this model is for honeycomb and foam materials with real anisotropic behavior. A nonlinear elastoplastic material behavior can be defined separately for all normal and shear stresses. These are considered to be fully coupled.

#72, Concrete Damage

This model has been used to analyze buried steel reinforced concrete structures subjected to impulsive loadings.

Author's note: This is the same model as Model 45 in DYNA. The LS-DYNA version reverts to an older version of Model 45 when all properties are entered. This model was developed in support of the Defense Threat Reduction Agency (DTRA, formerly Defense Nuclear Agency) programs.

Plastic flow is governed by a failure surface whose compressive meridian is determined in part by two of the three functions: initial yield surface, maximum failure surface, and residual failure surface. The program supports the controlling of the damage through a curve input. Element elimination is allowed. This model is used extensively in analyses of nonlinear continuum problems and is described in more detail in the next section.

#96, Brittle Damage

This is an anisotropic brittle damage model designed primarily for concrete but can be used for a wide variety of brittle materials. It permits progressive degradation of tensile and shear strengths across smeared cracks that are initiated under tensile loadings. Compressive failure is governed by a simplistic flow correction that can be disabled if not desired. Damage is handled by treating the rank 4 elastic stiffness tensor as an evolving internal variable for the material.

Model 193 (from LS/DYNA3D Manual)—Detailed Description

Material Type 193 is available in LS-DYNA. As noted, this model is a Group I model; thus it does not allow postfailure modeling or strain rate effects. However, the limited number and simple interpretation of input parameters make this model a good choice for comparison to results from other computer codes, or more simplified analysis.

The model is based on a Drucker-Prager formulation, but parameters for the yield surface are calculated from standard geotechnical parameters, namely c and N . The yield surface shape can be distorted by the failure surface shape parameter, RKF , and input variable. The soil parameters of G , ϕ , c , N , and ψ may be varied with depth, using a gradient that is part of the input parameters. Guidance or reference values for finding these parameters were discussed previously in the chapter on FLAC.

Model 16 (from DYNA3D Manual)—Detailed Description

Material Type 16 was initially developed to give concrete and geological material modeling capabilities to DYNA3D. It can be used in two major modes—a fairly simple tabular pressure-dependent yield surface, and a potentially complex model featuring two yield-versus-pressure functions with various means of migrating from one curve to the other. For both modes, load curve is taken to be a strain rate multiplier for the yield strength. Note that this model must be used with Equation of State type 9 or 11.

Equation of State types provide input for changes in properties as an analysis is in progress. Equation of State 9 allows a tabular relationship to be input that relates volumetric strain and pressure due to loading and temperature. Equation of State 11 allows the behavior to distinguish between a virgin loading curve and properties if the material is partially or completely crushed.

Response Mode I—Tabulated Yield Stress versus Pressure (Mohr-Coulomb)

This mode is well suited for implementing standard geologic and geotechnical models like the Mohr-Coulomb yield surface with a Tresca limit, as shown in figure 7. Examples of converting conventional triaxial compression data to this type of model are found in Desai and Siriwardane (1984). Note that under conventional triaxial compression conditions, the DYNA3D input corresponds to an ordinate of $(F_1 - F_3)$ rather than the more widely used $(F_1 - F_3)/2$ where F_1 is the maximum principal stress and F_3 the minimum principal stress. Using Material Type 16 combined with Equation of State Type 9 (saturated) or Type 11 (air filled porosity), has been successfully used to model ground shocks and soil/ structure interactions at pressures up to 100 kbar (approximately 1.5×10^6 lb/in²).

Simple Tensile Failure

Compression is controlled by a Mohr-Coulomb failure surface with a maximum cutoff. Tension failure is controlled by a cutoff value.

Response Mode II—Stress Strain Curve Input

Alternatively, this model may be used with two curves, a maximum yield strength curve, and a failed material curve. Damage and movement between the curves is controlled in one of three manners:

1. *Simple tension failure*—In this case, the yield strength is taken from the maximum yield curve until the maximum principal stress exceeds the tension cutoff. A proportional distance is taken between the 2 curves over 20 time steps until the minimum curve is reached.
2. *Tensile failure plus plastic strain scaling*—Uses an input table to define a damage scaling factor with plastic strain. This input allows hardening and/or softening.

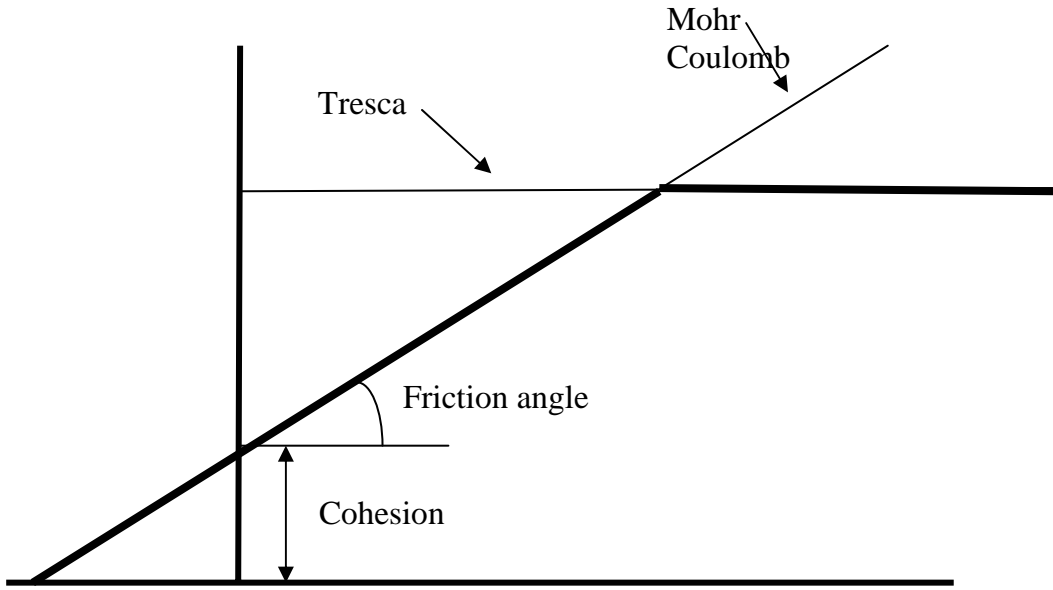


Figure 7.—DYNA Mohr-Coulomb / Tresca failure criterion.

3. *Tensile failure plus damage scaling*—Uses an input table similar to 2 but uses a prescribed damage function, rather than simply using plastic strain.

Model 45 (DTRA Concrete/Geological Material)— Detailed Description

Model Type 45 was specifically developed to ensure that material response follows experimental observations of standard uniaxial, biaxial, and triaxial tests for both tension and compression. This model depends on four sources of information for formulation of the stiffness and failure evaluations:

1. Equation of State—Bulk Modulus versus Volumetric Strain
2. Nested Plasticity curve fits of stress strain for:
 - Maximum stress
 - Yielding stress
 - Residual stress
3. Damage curve—function of plastic strain to move through nested surfaces
4. Rate effects curve of strength ratio versus strain rate

Equation of State

The equation state is input as a table (piecewise linear) of values of pressure versus volumetric strain (see fig. 8). Poisson's ratio is input as a parameter. Note

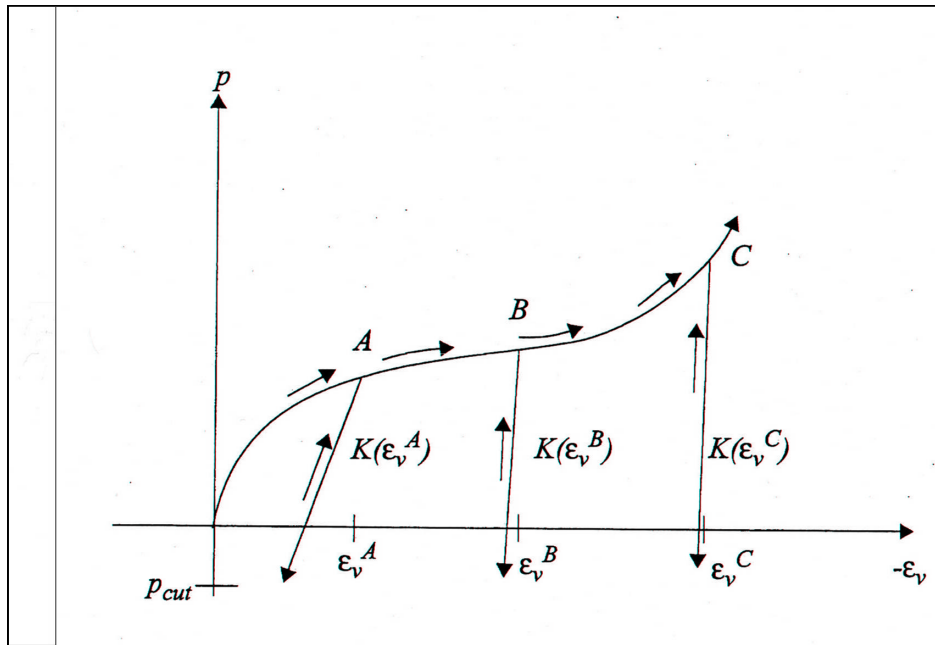


Figure 8.—Pressure vs. volumetric strain curve.

that unload-reload tests are required to find the bulk modulus at varying values of pressure and volumetric strain.

Plasticity Curves

The plasticity surfaces are input using three constants generated from a polynomial fit of laboratory stress-strain data (see fig. 9). The input variable names are as follows (Note: there is no cohesion-axis offset for residual strength):

1. Maximum surface
 - a-0 Cohesion of maximum failure surface
 - a-1 Coefficient for curve fit
 - a-2 Coefficient for curve fit
2. Yielding surface
 - a-0y Cohesion for initial yield surface
 - a-1y Coefficient for curve fit
 - a-2y Coefficient for curve fit
3. Residual surface
 - a-1f Coefficient for curve fit
 - a-2f Coefficient for curve fit

The shape of the nested curves is shown in figure 10.

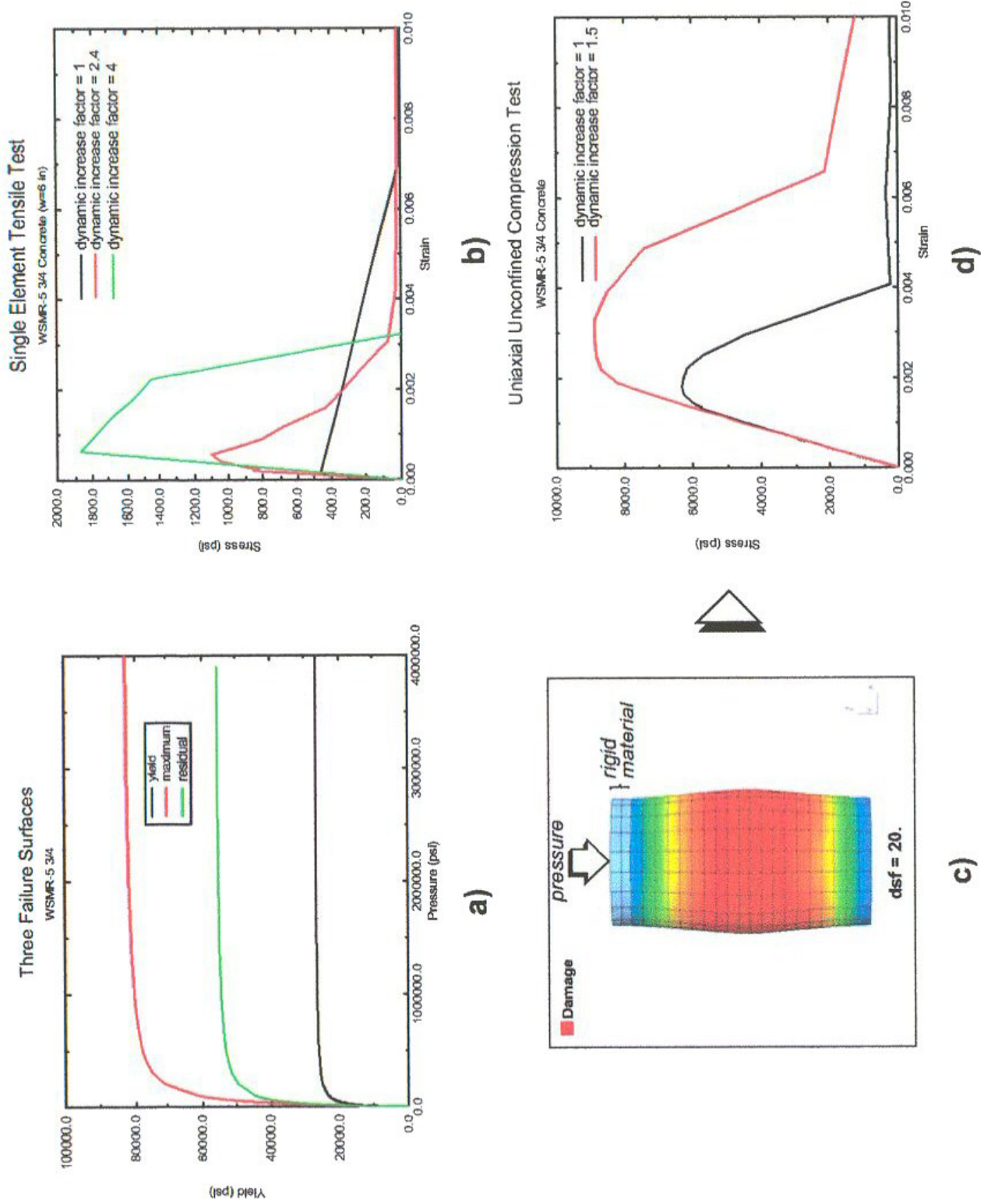


Figure 9.—(a) Nested Plasticity surfaces. (b) and (d) Rate Effects. (c) Typical model of a cylinder.

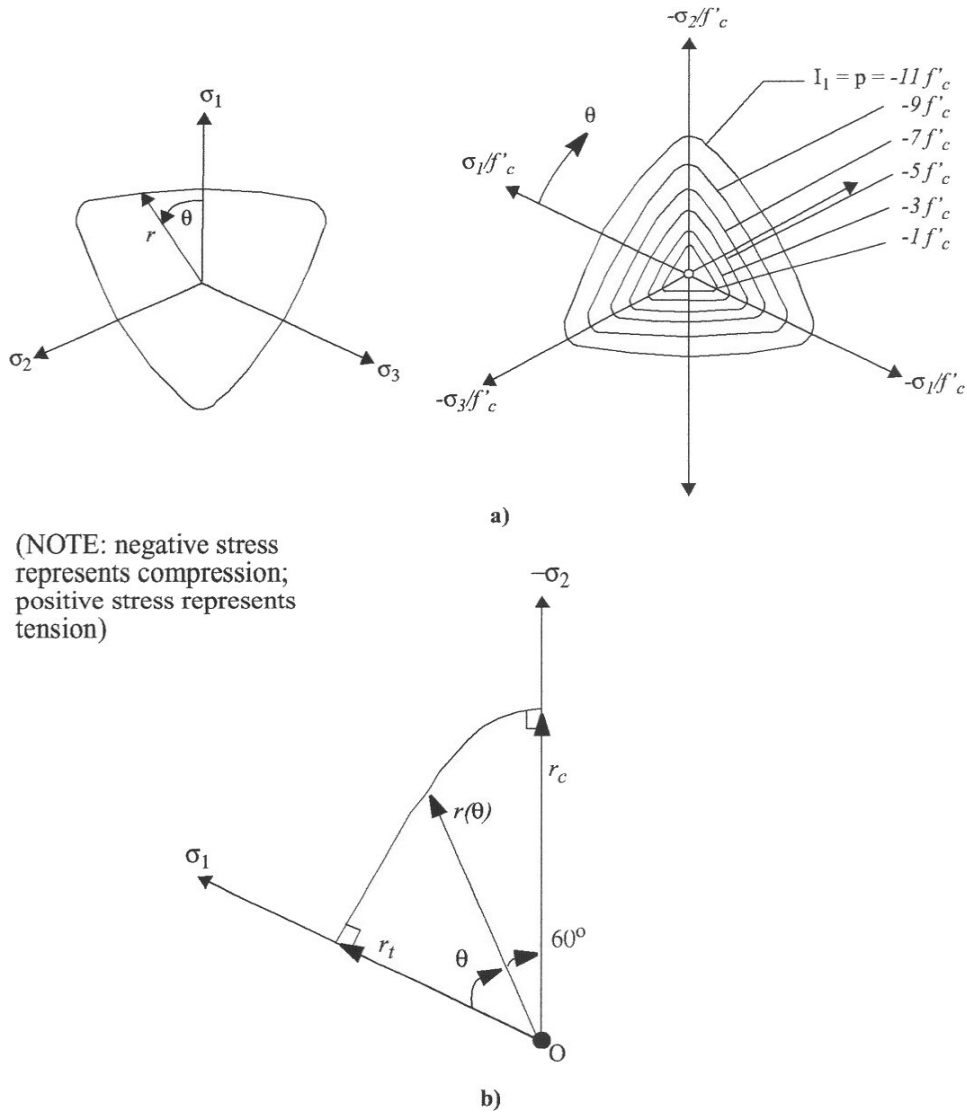


Figure 10.—Nested Plasticity Surfaces in DYNA

Uniaxial Tension Strength

Ultimate tensile strength is entered as a parameter. Once the stress reaches the tensile strength, damage evolution is used in tension.

Damage Evolution

The evolution of plasticity in compression and tension cutoff in tension are controlled through a tabular (piecewise linear) entry of the damage parameter fit as a function of the plastic volumetric strain (see fig. 11). Coefficients control the rate of the evolution for tension and compression as follows:

- b-1 Compression damage scaling coefficient
- b-2 Tension damage scaling coefficient (see fig. 12)
- b-3 Tension damage scaling coefficient adjusted for triaxial tension

Lambda, Nu

WSMR	Lambda	Nu
	0	0
	1.00E-05	0.85
	3.00E-05	0.96
	5.00E-05	0.99
	7.00E-05	1
	9.00E-05	0.99
	1.10E-04	0.96
	2.70E-04	0.5
	5.80E-04	0.05
	7.80E-04	0.01
	1.33E-02	0
	5.00E-01	0
	6.00E-01	0
SAC	Lambda	Nu
	0.00E+00	0
	1.50E-04	1
	2.80E-04	0.24
	1.20E-03	0
	1.00E-01	0
	2.00E-01	0
	3.00E-01	0
	4.00E-01	0
	5.00E-01	0
	6.00E-01	0
	7.00E-01	0
	8.00E-01	0
	9.00E-01	0

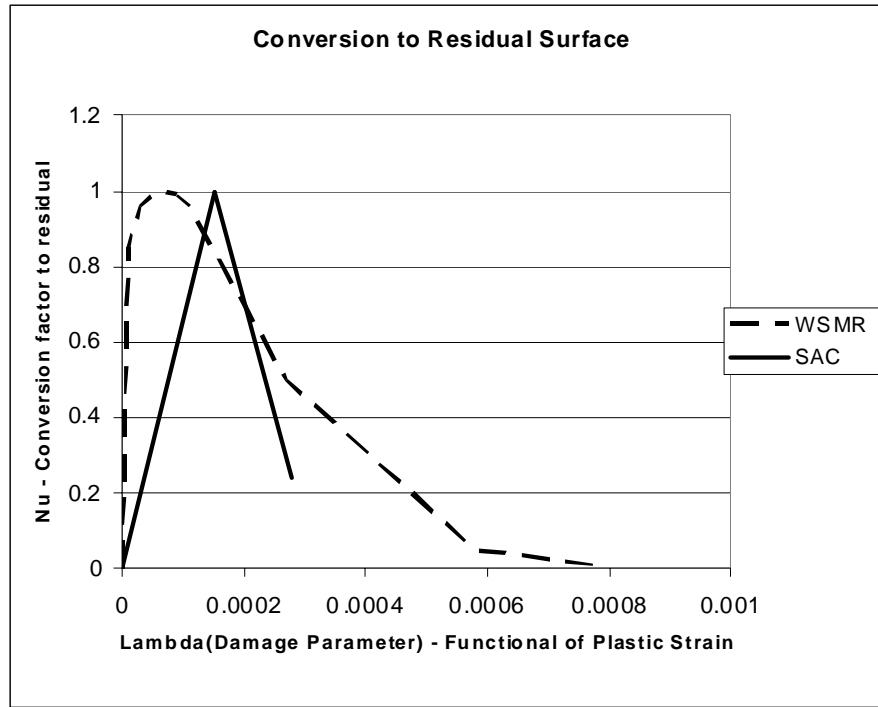


Figure 11.—The evolution of plasticity in compression and tension cutoff in tension controlled through a tabular (piecewise linear) entry of the damage fit as a function of the plastic volumetric strain.

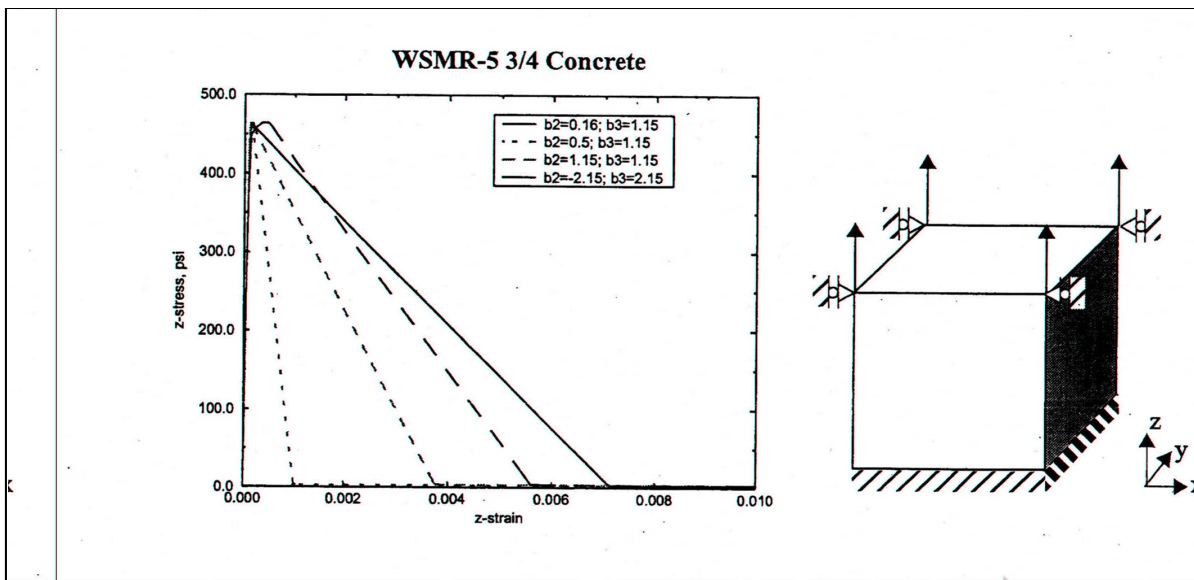


Figure 12.—Effects of parameters b_2 and b_3 on softening for a single element tensile test.

Typical values found for the a and b coefficients for the so-called White Sands (WSMR) and SAC concretes are shown in table 11. At Reclamation, these parameters can be calculated using *Materials Properties for Nonlinear Finite Element Analysis* (Harris and Madera, 2004).

Table 11.—Typical values found for the a and b coefficients for WSMR and SAC concretes

Type	A ₀	a ₁	a ₂	a _{0y}	a _{1y}	a _{2y}	a _{1f}	a _{2f}	b ₁	b ₂	b ₃
WSMR	1834	0.491	0.000013	1385	0.625	0.000032	0.4417	0.000019	1.5	1.6	1.15
SAC	2442	0.33	0.000011	1738	0.7414	0.000000	0.4417	0.000016	1.4	1.5	0.4

Shear Dilation

Shear Dilation is allowed in the model. Dilatancy in this sense is the effect of sliding surfaces needing to clear jagged planes created by aggregate extrusions into the plane (see fig. 13). Once the gap is sufficiently open to clear these jagged peaks, the dilatancy no longer occurs. A factor, w , is used to vary this effect. This parameter can be reasonably estimated, and typical concrete experiments show it to be between 0.5 and 0.7. The value of the parameter ranges from 0, which implies no change in volume during plastic flow, to 1, which implies shear dilation during flow. The dilatancy decay can also be controlled by the parameter, $edrop$, which varies from 1 (a linear drop to zero), to a large number (a rapid drop). Rate effects are also allowed in the damage effect relationship using the input parameter, s .

Element Elimination

Elements, which exhibit large volumetric deformation following failure, can be eliminated from the calculations (i.e., can carry no stress) using a maximum volumetric strain as input.

Strain Rate Effects

The effect of strain rate is entered as tabular (piecewise linear) data for compression and tension effects. Data for concrete tests of typical concrete pavements are shown in figure 14. Strain rate data for embankment materials are not readily available and need to be developed.

To summarize the tests needed for a full description of parameters, a full suite of tests would include (see table 12):

- Standard uniaxial compression with axial and lateral measurements
- Uniaxial compression unload/reload with axial and lateral measurements and post peak data

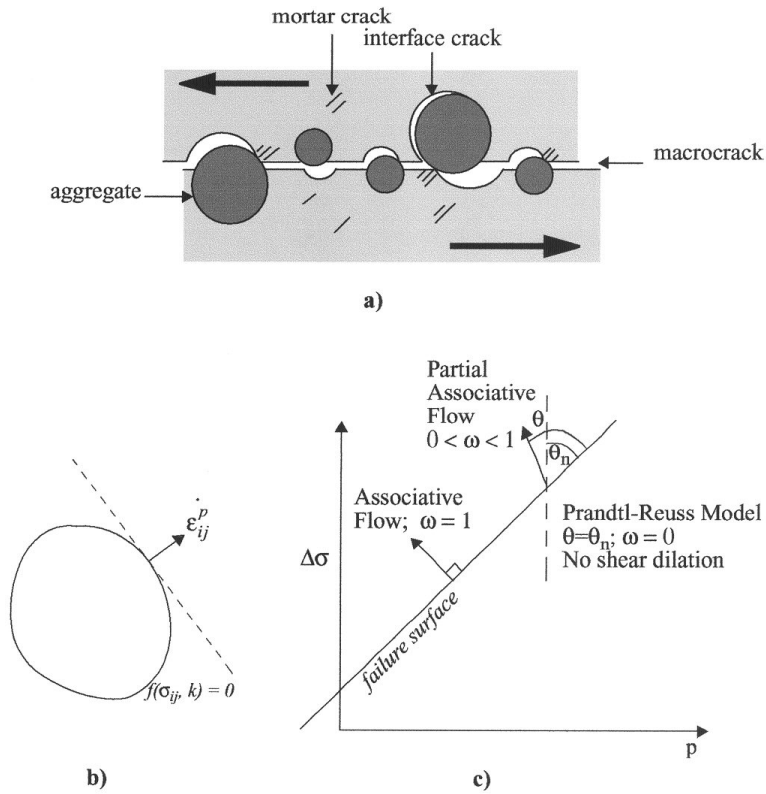


Figure 13.—(a) Graphical representation of shear dilation (b) Yield surface with associated flow rule (c) Description of associative, nonassociative, and partial flow rules.

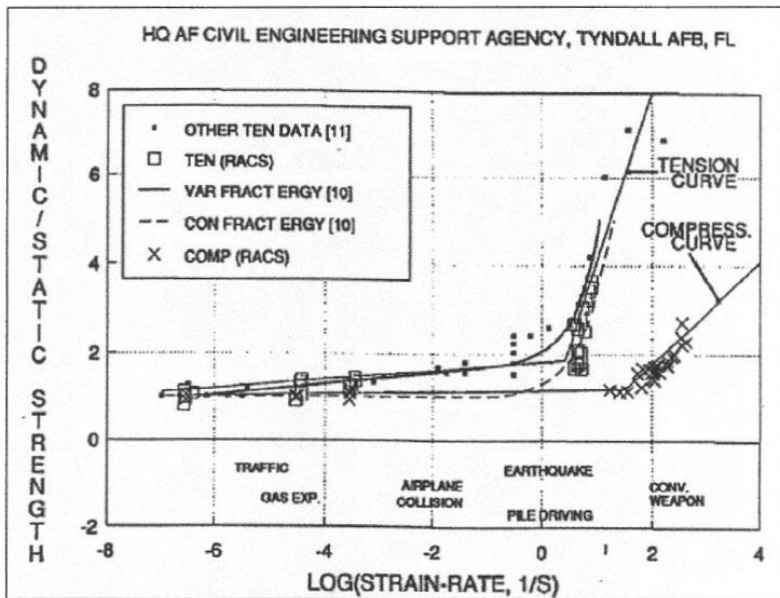


TABLE 19. DYNA3D input

Strain Rate	Strength Factor
-1.000E+02	7.960E+00
-1.000E+01	4.040E+00
-1.000E+00	1.890E+00
-1.000E-01	1.780E+00
-1.000E-02	1.670E+00
-1.000E-03	1.560E+00
0.000E+00	1.000E+00
1.000E-03	1.119E+00
1.000E-02	1.150E+00
1.000E-01	1.200E+00
1.000E+00	1.300E+00
1.000E+01	1.375E+00
1.000E+02	2.000E+00
1.000E+03	3.000E+00

Figure 14.—Strain rate effects on tensile and compressive strengths.

Table 12.—Parameter and testing requirements for DYNA-3D

Stress state	Parameter	Recommended test	Needed data
Elastic	K, bulk modulus G, shear modulus	Uniaxial compression test with axial and circumferential strain gauges	K: stress vs. volumetric strain G: shear stress vs. shear strain Alternate data E: Axial stress vs. axial strain PR: Lateral strain vs. longitudinal strain
Failure Plasticity surfaces	Curve fit coefficients to stress-strain	Uniaxial compression test with axial and circumferential strain gauges	Family of stress-strain curves
Cutoff values	Tension strength cutoff Maximum volumetric strain	Static direct tension Split cylinder	Tensile strength Maximum volumetric strain
Damage evolution	Lambda, Nu curve b, coefficients for damage evolution	Unload-reload tests Static direct tension	
Rate effects	Rate table input	Dynamic compression Dynamic split tension	Ratio dyn/static

- Direct tension with axial and lateral measurements
- Direct tension w unload/reload and post peak measurements
- Split cylinder
- Dynamic uniaxial compression
- Dynamic split cylinder

Data for rate effects on soil parameters have not been found in an exhaustive literature search. Some testing to confirm the effect of strain rates on soils needs to be conducted.

LSDYNA or DYNA Dynamic Pore Pressure Calculations

LSDYNA and DYNA do not have a direct method for the calculation of pore pressures or increase of pressures during dynamic events of soils. Such events

would need to be incorporated through the material input. Note that the Equation of State input does allow saturated and nonsaturated materials. Alternatively, a liquefied layer could be assumed or implied by another method, and this layer could be modeled as a low strength material and the deformations calculated as a check.

Author's note: Model 45 in DYNA, due to its emphasis on properties found from standardized testing, is recommended as a first choice for nonlinear analysis of concrete and can also be used for soil and rock when stress-strain data are available to find the input parameters. If LS-DYNA is to be used as the computational tool, Model 16, Model 78, or Model 193 is recommended for soils and rock. The calculation of parameters for Models 16 and 78 is similar to that for Model 45, while the calculation of Model 193 parameters is more similar to that for FLAC, using c and N_f for the initiation of failure. The choice of model would depend on the more reliable data available for input.

Use of Damping in Analysis

Damping is required in all dynamic analyses. Damping represents the resistance to deformations when velocities are present. The damping can be either from materials effects or the hysteresis energy consumed by the unloading and reloading of the material, or it may be inertial, the resistance to deformation due to the mass of the structure subjected to accelerations, or both. Using a coupled analysis with material and structural damping requires much longer computation times in computer analyses than a simpler material damping only.

A coupled analysis uses what is generally referred to as Rayleigh damping. In this formulation, a coefficient, α , is used as the variable controlling the inertial or contribution from the mass. Similarly, a coefficient, β , is used, controlling the material or stiffness influence. In this formulation, the mass contribution controls at low frequencies, while the stiffness contribution controls at higher frequencies. An example of a Rayleigh estimate compared to data from embankment dams is shown in figure 15. Note that in this graph, the Rayleigh coefficients are $\alpha = 0.4$ and $\beta = 0.0002$.

The FLAC Optional features manual suggests using material damping initial computer runs with a final check of the analysis using mass damping as well. In many cases, the material damping only will provide reasonable results. Material damping is readily found using standard laboratory tests. In cases where it is clear that the inclusion of mass damping is required, due to major changes in the answers, additional runs will be required, but the effects of a full variation of parameters may not be necessary, still saving overall effort in the analyses.

Half Band Damping Estimates

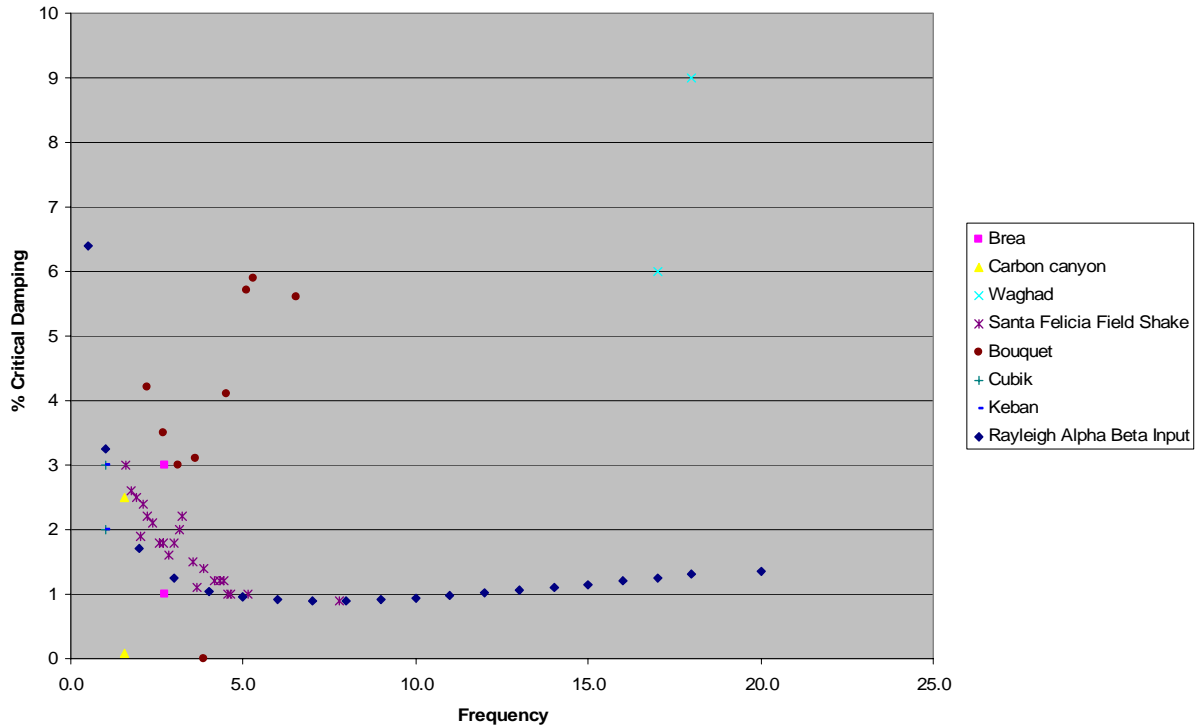


Figure 15.—Embankment dam damping data and Rayleigh equation estimate for damping.

The suggestion that material-only damping may be sufficient relies on two structural principles: (1) the dam may not respond to lower frequencies where mass damping is most prevalent, or (2) the input motion of the earthquake may not contain significant energy inputs in the spectra that will excite any lower frequencies. Data from on-site shaker tests (described later) or back-calculated from earthquake records is shown in figure 16. From these data, it is clear that there is a wide variation in the fundamental structural response mode where dams with lower frequencies will need mass effects to be considered, and dams with higher fundamental frequencies may not. Rather than using a trial-and-error approach, with judgment, on critical structures, it is recommended that field measurements be made to ensure that the proper structural and material effects are included. Note that in either case, material damping is required.

Material Damping

Material damping is calculated from typical cyclic or resonant column tests. The damping is generally described as a percent damping with the calculation being governed by ASTM D-3999, *Standard Test Methods for the Determination of the Modulus and Damping Properties of Soils Using the Cyclic Triaxial Apparatus*, and ASTM D-4015, *Standard Test Methods for Modulus and Damping of Soils by the Resonant-Column Method*.

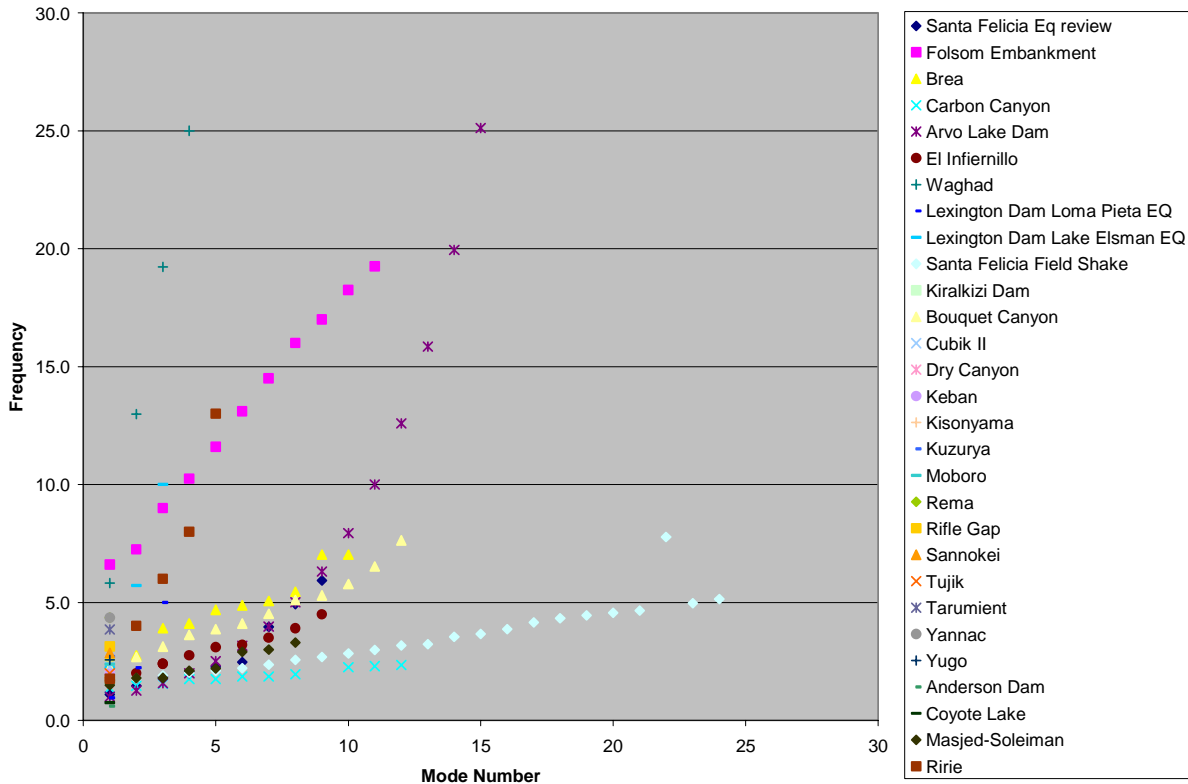


Figure 16.—Typical frequencies of embankment dams.

The Cyclic Triaxial approach utilizes the unload-reload portion of a test to report damping from the ratio of the hysteresis loop area with a measure of the elastic area of the energy under the loop as shown in figure 17.

Data for cyclic soil tests and the calculated damping (Roblee and Chiou, 2004) are shown in figures 18 through 20. These data also show that the effect of the soil type on the damping ratio is fairly significant as shown in figure 21. For this reason, default values in computer codes should not be used, and empirical or typical values should be considered carefully before use. Using damping curves that show too much damping for the material chosen would not be conservative because the damping coefficient resists deformation under dynamic loading. Values such as those shown may be useful for preliminary studies; however for decisions related to proving a low risk to the public, to design, or to preparing a budget for Congressional approval, actual measured values from the structure in question are recommended.

Structural Damping

Structural damping may be measured directly in the field using an eccentric shaker. This procedure is established in Reclamation and has been used on concrete dams. The shaker can energize the structure at different frequencies. From the response of the structure, both structural response frequencies and the

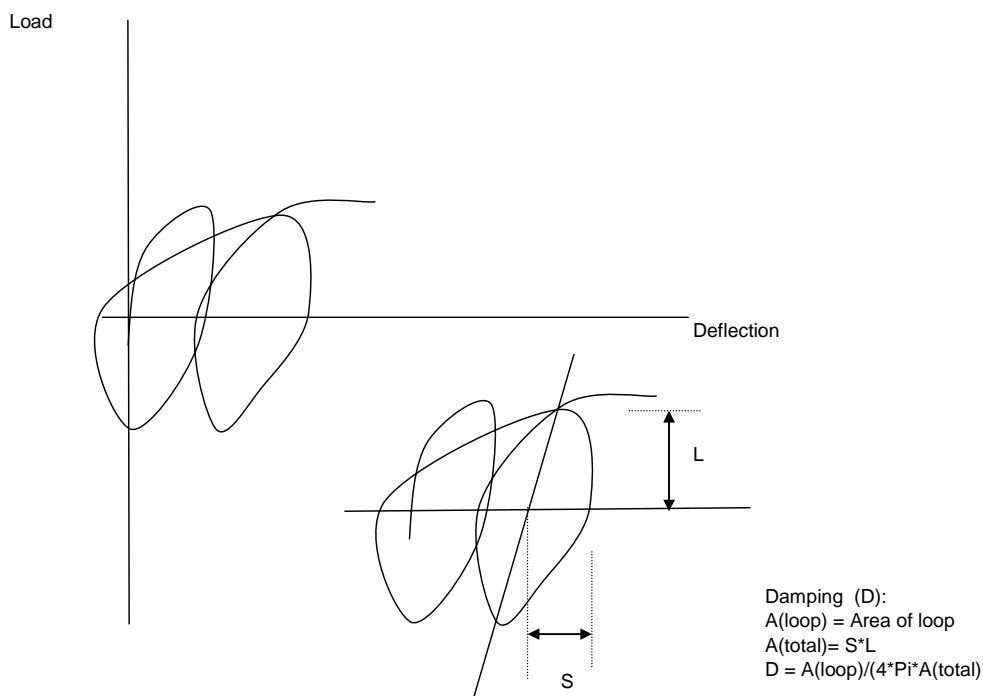


Figure 17.—Calculation of damping from material hysteresis.

associated damping with the frequencies can be found. Example data for frequencies for concrete dams are shown in figure 22.

Recent work (Duran et al., 2005) shows that representative values may be obtained in embankments using the same techniques. In this work, a stake driven into the ground was used with an accelerometer attached for the accelerometer instrumentation. The shaker was attached to the concrete dam main section, with data taken from the accompanying embankment. In other work, data from an eccentric shaker used to energize an embankment dam is presented (Gupta, et al., 1980) In this field application, a 1.5- by 1.0- by 1.5-meter block of concrete was embedded firmly in the top of the embankment and used as a shaker base. This method provided excellent data. Other measurements taken in embankment dams (Keightley, 1966) used an 8- by 24-foot, 16-inch thick slab cast into the dam and capable of holding two eccentric vibration systems creating a maximum force of 5,000 pounds per machine. Data for embankment dams are not as extensive; example data were shown in figures 18 through 20.

The damping of the structure can be estimated from the response data using the half-power bandwidth method. A damping factor is calculated for each resonant frequency and direction of excitation. In some cases, the damping cannot be calculated because the resonance is not well defined, that is, the magnitude does not have a sharply defined peak. Table 13 lists the estimated damping factors for the major resonances during a field shaking of East Canyon Dam (concrete).

Computer Material Models for Soils Using FLAC and DYNA

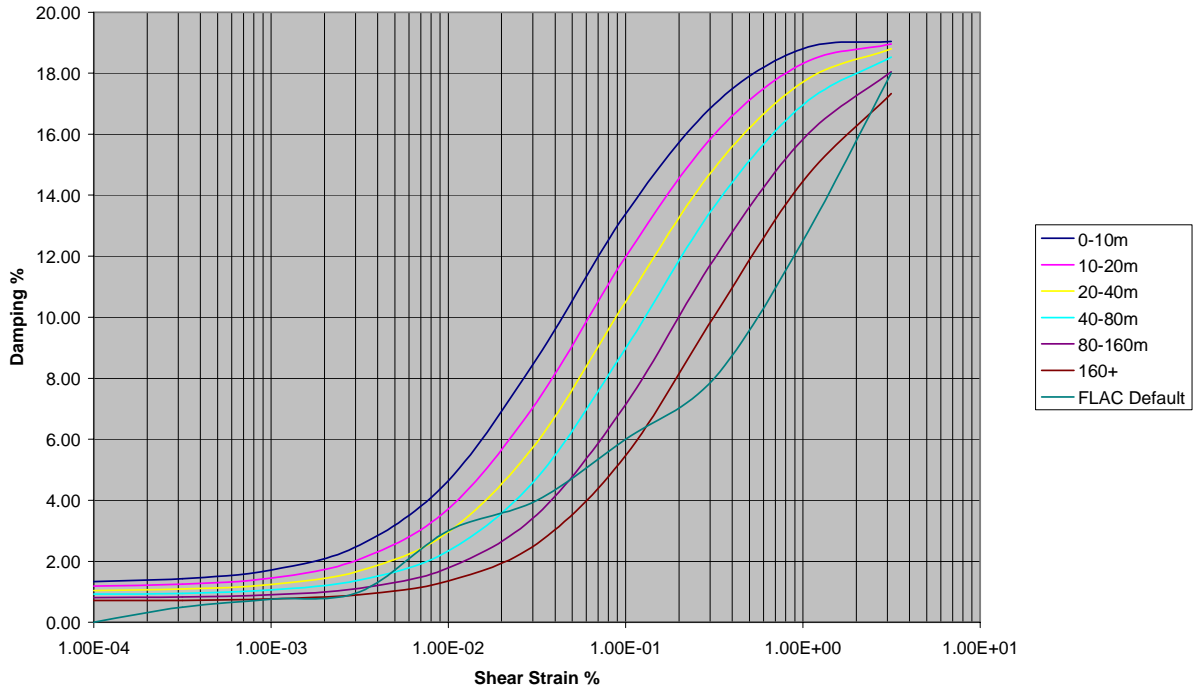


Figure 18.—Damping ratio by depth for primarily coarse materials.

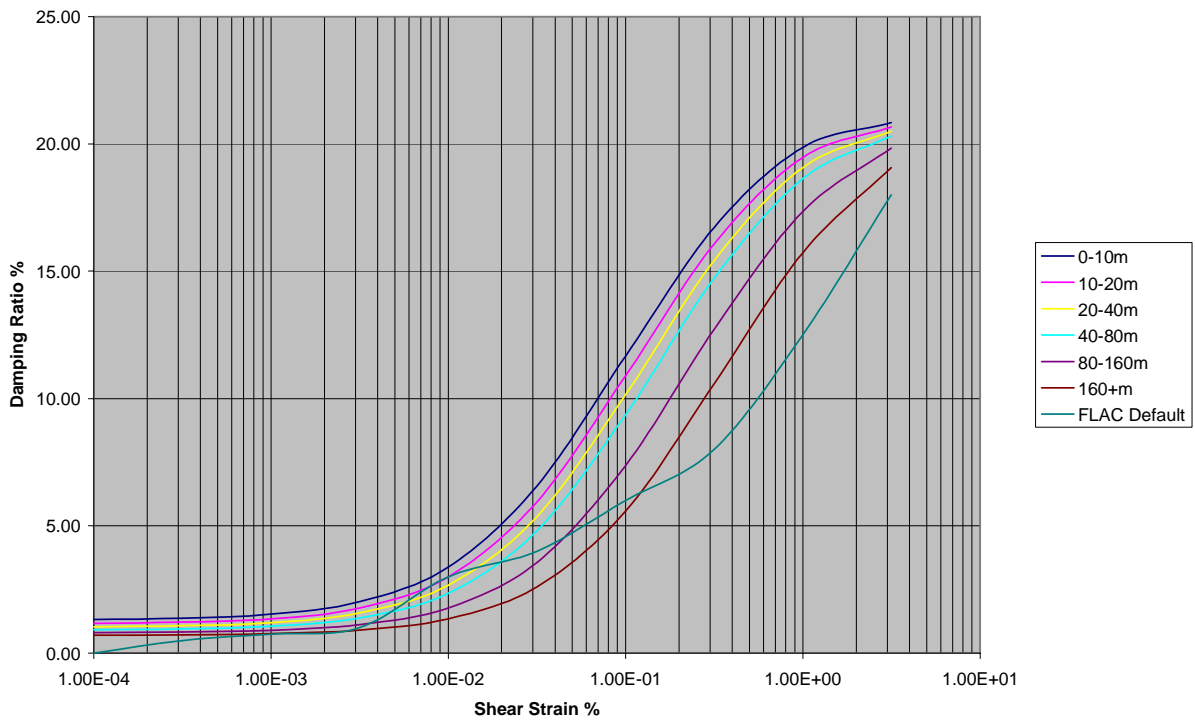


Figure 19.—Damping with depth for fine grained soils with low plasticity index.

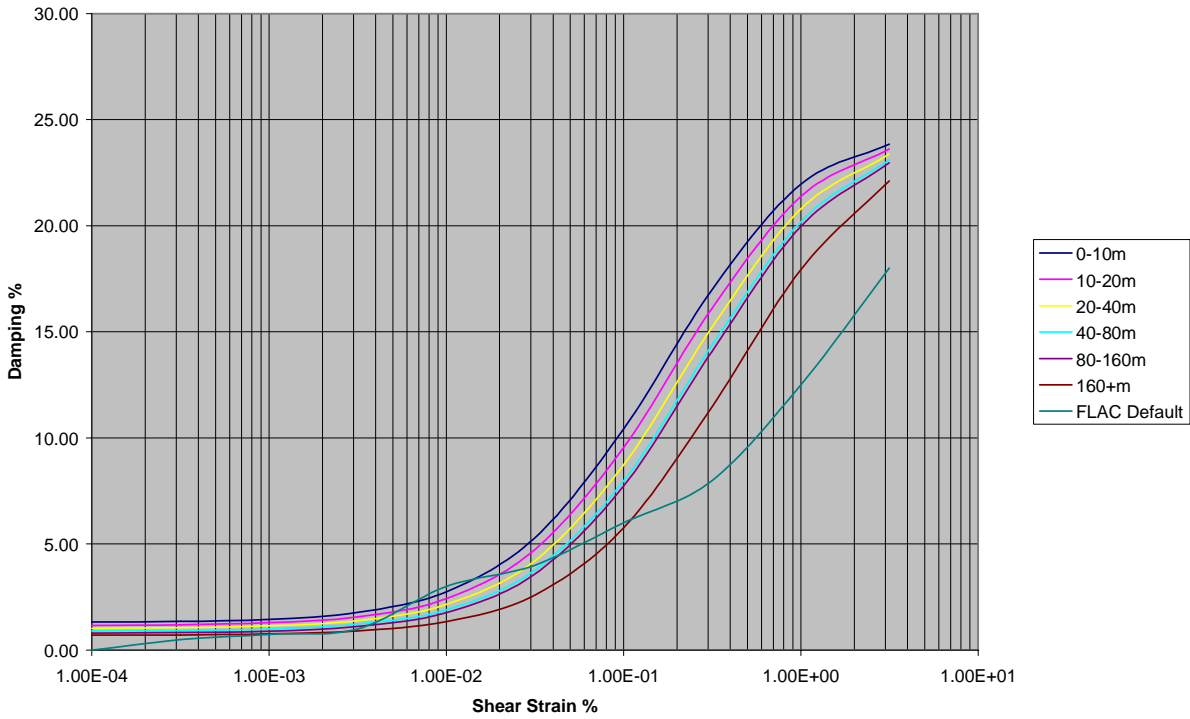


Figure 20.—Damping with depth for fine grained, high plasticity materials.

**Soil Types - 20 to 40 m
Damping ratio**

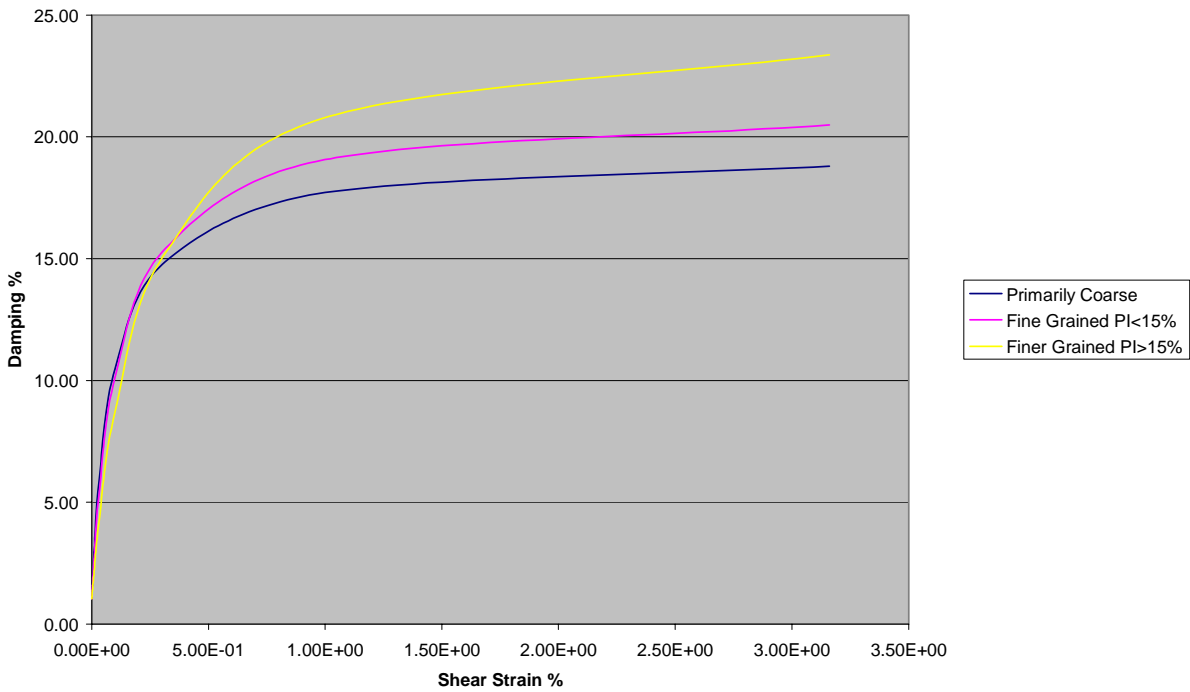


Figure 21.—Effect of soil type on damping ratio.

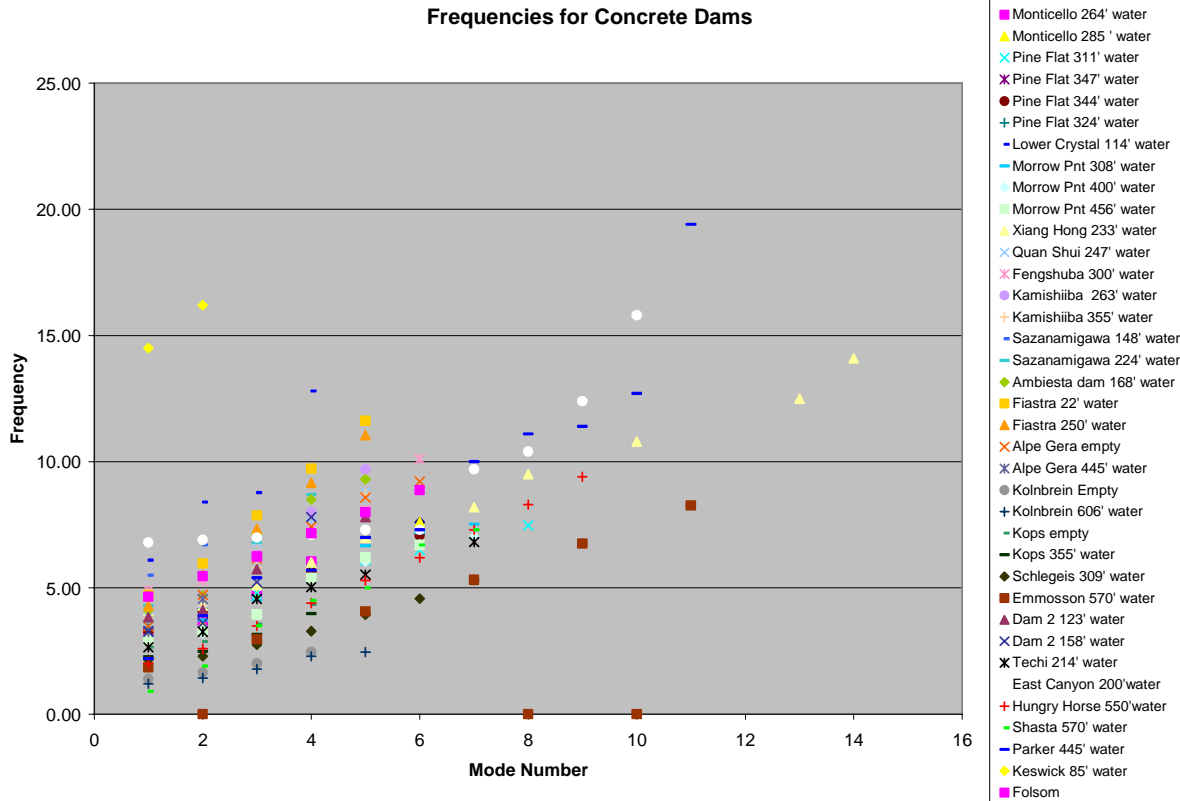


Figure 22.—Typical frequencies of concrete dams.

The half-power bandwidth method for estimating damping uses the following formula:

$$\text{fraction of critical damping} = \Delta f / (2 * f_N)$$

where,

Δf = width of the magnitude curve at the resonant frequency half-power point

f_N = resonant frequency

The calculation is illustrated in figure 23 for a resonance at 5.7 Hz. The value of the peak at the resonant frequency is read from the graph (or the data used to generate the graph). This is multiplied by $\sqrt{2}/2$, or 0.707, to obtain the half-power point. The width of the magnitude curve at the half-power point is read from the graph. The figure shows the peak magnitude at the resonant frequency to be 0.00042, and the calculated half-power point as 0.000297. The width of the curve at the half-power point is seen to be 0.25 Hz, which is Δf . Applying the above formula yields the fraction of critical damping to be 1.9 percent.

Table 13.—Estimated damping factors for prominent resonant frequencies

Test site	Excitation direction	Resonant frequency (Hz)	Percent of critical damping
S1	U/D	6.8	4.4
S1	U/D	7.3	3.9
S1	U/D	10.4	4.0
S1	U/D	12.4	2.7
S1	U/D	15.8	2.5
S1	C-C	6.9	4.8
S1	C-C	7.0	4.3
S1	C-C	7.1	3.4
S1	C-C	7.3	4.9
S1	C-C	9.7	2.5
S2	U/D	6.8	3.1
S2	U/D	9.2	2.7
S2	U/D	9.5	3.7
S2	U/D	11.8	2.9
S2	U/D	14.7	2.1
S2	U/D	17.8	2.0

Forced vibration tests for concrete dams has been ongoing for some time, and data are readily available (Hall, 1988) for many sites as shown in figure 24. These data do show the considerable range over which the damping ratio can occur. Data for embankment dams are less common. Example data were shown in figures 18 through 20. Because data are sparse, the use of previous values for precedent is not recommended. Damping values used in nonlinear analysis need to be carefully reviewed to confirm that damping alone does not create unrealistic results.

Conclusions and Recommendations

1. For decisions related to proving a low risk to the public, to design, or to preparing a budget for Congressional approval, the best set of analyses to study various possible loadings and investigate various possible failure scenarios with a range of assumptions needs to be completed. Actual measured values from the structure in question are recommended.

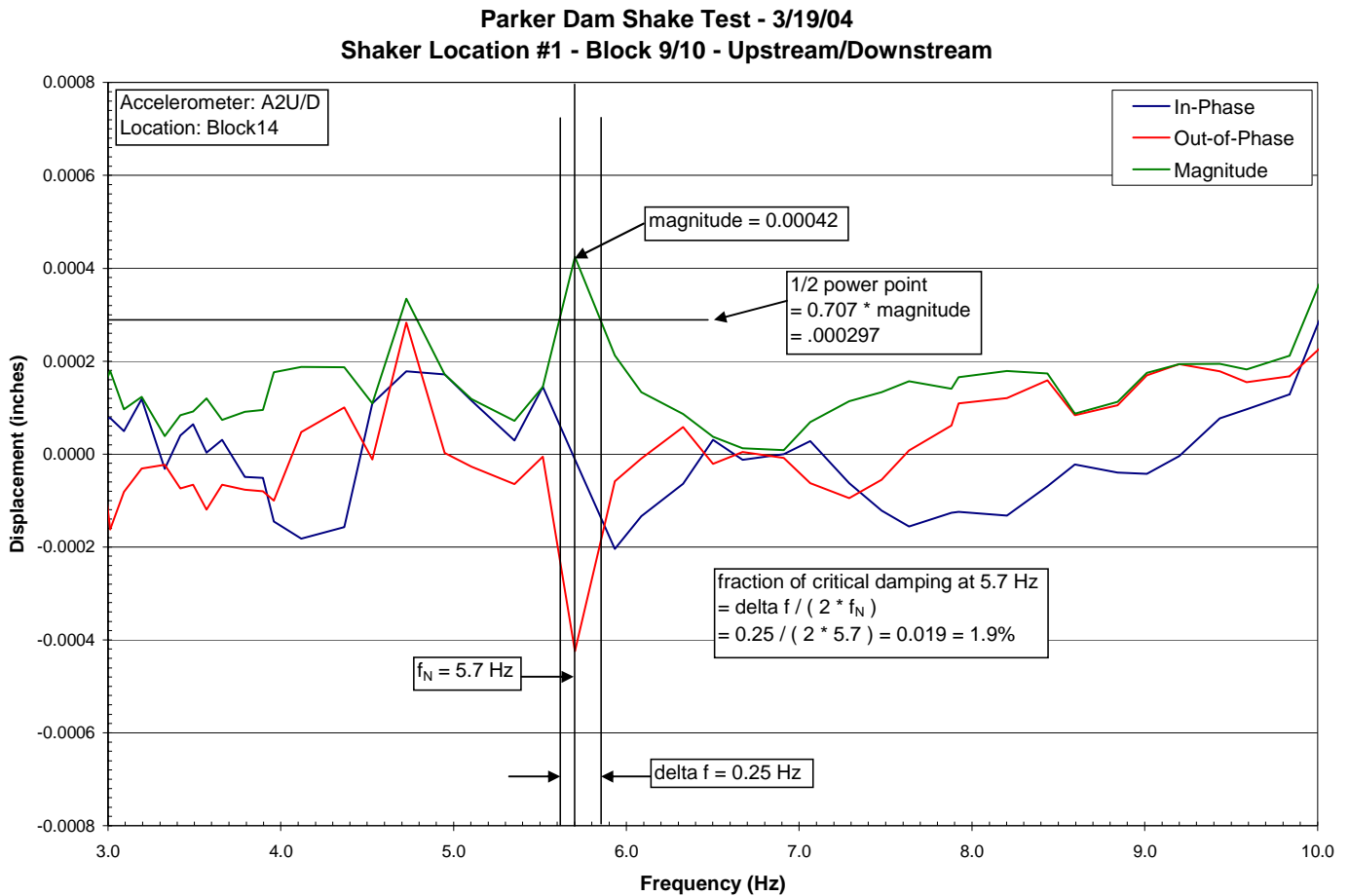


Figure 23.—Example calculation of structural damping using a field shaker.

2. Linear properties have been used in analysis and stresses compared to failure values. The inherent problem in this approach is that materials do not act in a linear fashion to their failure point. The approximation may be justified if the stresses in the soil mass are far from failure, if the changes in stress are small, and the magnitudes of the deformations are not of critical interest. In cases where these conditions are not met, nonlinear analyses should be incorporated into the state of the practice for evaluating site response to better understand the uncertainties in nonlinear soil behavior and assess their impact. Nonlinear analyses provide a more realistic approach for evaluating the impact of strong ground shaking on soft, potentially liquefiable soils, and their effects on estimated ground motions on the surface of these deposits.
3. FLAC and DYNA have the capability to model linear and elastic conditions, as well as failure and postfailure conditions. These computer codes or their equivalent should be used to perform state of the practice nonlinear analyses on critical structures under evaluation.

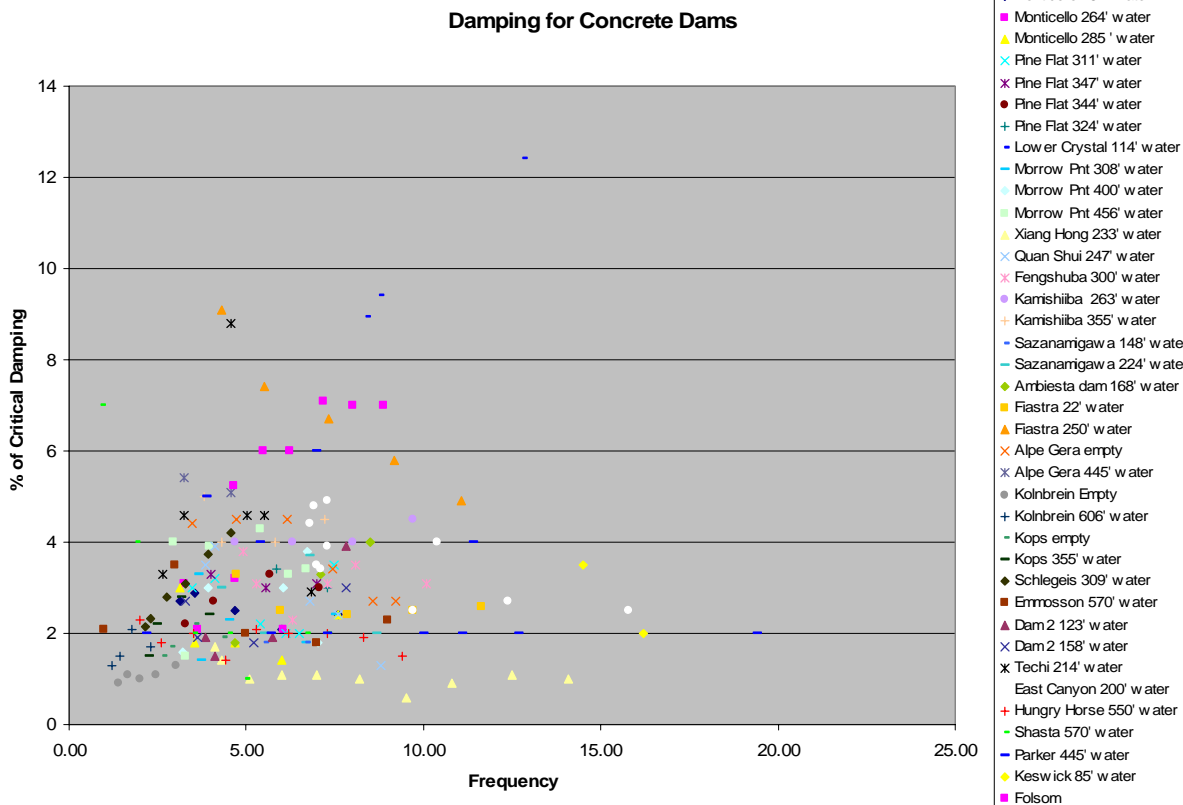


Figure 24.—Damping characteristics for various concrete dams.

4. Material models have been developed that allow input parameters to be measured from samples and can account for varying properties on different projects.
5. Conventional triaxial tests should be used in testing series and volumetric measurements made to permit calculation of parameters. Unload-reload tests should be done to allow moduli to be calculated for various stress conditions and to allow plastic parameters to be calculated at typical and high levels (10%) of strain.
6. Dynamic soil tests using either cyclic or resonant column tests need to be used for cases where earthquake loadings are being studied. Laboratory tests provide the fundamental material properties used in analysis without the use of empirical or estimated correlations. In-situ tests can be used to provide a continuous log of soil layers and to be used where sampling cannot be accomplished on fragile, liquefiable soils.
7. Postliquefaction strength of soils is not fully understood. The data supporting SPT strength correlations are few and of variable quality. Because both laboratory test measurements and correlations with *in situ* properties

have serious drawbacks, neither approach can be considered a definitive indication of the available strength. The uncertainty in strength estimates must be acknowledged, and sensitivity to variations in strength must be analyzed.

8. Better experimental data for volume changes during complicated cyclic loading paths are needed. Pore pressure models can then be revised accordingly.
9. Strain rate tests on soils need to be pursued to ascertain the extent that this effect has on observed behavior.
10. Material stiffness and material damping curves versus shear strain levels need to be established for review of critical structures under dynamic conditions.
11. Dynamic modes need to be confirmed for critical structures to ensure that proper damping values are used.

References

- Byrne, P. 1991. *A Cyclic Shear-Volume Coupling and Pore pressure Model for Sand*. Paper 1.24. Proceedings Second International Conference on Recent Advances in Geotechnical Earthquake Engineering and Soil Dynamics. St. Louis, Missouri.
- D'Appolonia, D.J., E. D'Appolonia, and R.F. Brisette. 1970. "Settlement of spread footings on sand." *Journal of the Foundation Division*. ASCE. 96(SM2). pp. 754-761.
- Das, B.M., *Principles of Geotechnical Engineering*, 3rd Ed., PWS Publishing Company, 1994.
- Desai, C.S., and H.J. Siriwardane. 1984. *Constitutive Laws For Engineering Materials with Emphasis On Geologic Materials*. Prentice-Hall. Chapter 10.
- Duncan, J.M. and Kai Sin Wong. 1999. *User's Manual for SAGE*. Volume II "Soil Properties Manual." Center for Geotechnical Practice and Research. Virginia Polytechnic Institute and State University.
- Duncan, J.M. and C.Y. Chang. 1970. "Nonlinear analysis of stress and strain in soils," *Journal of the Soil Mechanics and Foundations Division*. ASCE. 96(SM5). pp. 1629-1653.

- Duncan, J.M. and Kai Sin Wong. 1999. *User's Manual for SAGE*. Volume II—“Soil Properties Manual.” Center for Geotechnical Practice and Research, Virginia Polytechnic Institute and State University.
- Duran, Z., E.E. Matheu, V.P. Chiarito, J.F. Hall, and M.K. Sharp. 2005. *Dynamic Testing and Numerical Correlation Studies for Folsom Dam*. Report ERDC/GSL TR-05-## (Draft), U.S. Army Corps of Engineers Engineering Research and Development Center.
- Harris, D.W. and V. Madera. 2004. *Materials Properties for Nonlinear Finite Element Analysis*. Materials and Engineering Research Laboratory. Bureau of Reclamation. Denver, CO.
- Goodman, R.E. 1980. *Introduction to Rock Mechanics*. John Wiley and Sons. New York.
- Gupta, S.P, L.S. Srivastava, P. Nandakumaran, and S. Mukerjee. 1980. “In-Situ Measurement of Dynamic Characteristics of an Earth Dam.” *Proceedings of the 7th World Conference on Earthquake Engineering*. Istanbul, Turkey.
- Hall, J.F. 1988. “The dynamic and earthquake behavior of concrete dams, review of experimental behavior and observational evidence.” *Computational Mechanics Publications*.
- Harder, L.F., Jr., and H.B. Seed. 1986. *Determination of Penetration Resistance for Coarse-Grained Soils Using the Becker Hammer Drill*. Report No. UCB/EERC-86-06. University of California Earthquake Engineering Research Center. Berkeley, CA
- Idriss, I.M. and J.I. Sun. 1991. *SHAKE91*. University of California. Davis, CA.
- Keightley, W.O. 1966. “Vibrational Characteristics of an Earth Dam.” *Bulletin of the Seismological Society of America*, 56(6). pp. 1207-1226.
- Livermore Software Technology Corporation. 2003. *LS-DYNA Keyword User's Manual*. Livermore, CA.
- Makdisi, F.I. and Z.L. Wang. 2004. “Nonlinear Analyses for Site Response — Opinion Paper.” *International Workshop on the Uncertainties in Nonlinear Soil Properties and their Impact on Modeling Dynamic Soil Response*.
- Martin, G.R., W.D.L. Finn, and H.B. Seed. 1975. “Fundamentals of Liquefaction Under Cyclic Loading.” *Journal of the Geotechnical Division*. ASCE. 101(GT5). 423-438.

Lin, Jerry I (Current Developer). 2002. *DYNA3D—A Nonlinear, Explicit Three Dimensional Finite Element Code for Structural and Solid Mechanics, User Manual*. Methods Development Group, Lawrence Livermore National Laboratory.

Livermore Software Technology Corporation. 2003. *LS-DYNA*. Livermore, CA.

Ortiz, J.M.R, J Serra, and C. Oteo. 1986. *Curso Aplicado de Cimentaciones*. Third ed. Colegio de Arquitectos de Madrid. Madrid.

Puebla, H., P.M. Byrne, and R. Phillips. 1997. “Analysis of CANLEX liquefaction embankments and centrifuge models.” *Canadian Geotechnical Journal*. (34). pp. 641-657.

Robertson, P.K. and R.G Campanella. 1983. “Interpretation of Cone Penetration Tests.” Parts I and II. *Canadian Geotechnical Journal*. 20(4). pp. 718-745

Roblee, Cliff and Brian Chiou. 2004. *A Proposed Geindex Model for Design Selection of Non-Linear Properties for Site Response Analyses*. International Workshop on Uncertainties in Nonlinear Soil Properties and Their Impact on Modeling Dynamic Soil Response, PEER Headquarters, UC Berkeley.

Seed, R.B. and L.F. Harder, Jr. 1990. “SPT-based analysis of cyclic pore pressure generation and undrained residual strength.” *Proceedings H. Bolton Seed Memorial Symposium*. Bi-Tech Publ. Ltd. Vol. 2, Vancouver, B.C. Canada.